Tidal notches in Mediterranean Sea: a comprehensive analysis

Fabrizio Antonioli [a], Valeria Lo Presti [b, a, *], Alessio Rovere [c, d], Luigi Ferranti [e], Marco Anzidei [f], Stefano Furlani [g], Giuseppe Mastronuzzi [h], Paolo E. Orru [i], Giovanni Scicchitano [j], Gianmaria Sannino [a], Cecilia R. Spampinato [k], Rossella Pagliarulo [l], Giacomo Deiana [i], Eleonora de Sabata [m], Paolo Sansò [n], Matteo Vacchi [o], Antonio Vecchio [f]

[a] *ENEA, UTMEA, Casaccia, Roma, Italy*
[b] *Department of Earth Sciences, "Sapienza" University, Rome, Italy*
[c] *MARUM, University of Bremen & ZMT, Tropical Marine Ecology Center, Bremen, Germany*
[d] *Lamont-Doherty Earth Observatory, Columbia University, NY, USA*
[e] *Department of Earth Sciences, Environment and Resources, "Federico II" University, Napoli, Italy*
[f] *Istituto Nazionale di Geofisisica e Vulcanologia, Roma, Italy*
[g] *Department of Mathematics and Geosciences, University of Trieste, Italy*
[h] *Department of Earth and Geoenvironmental Sciences, "Aldo Moro" University, Bari, Italy*
[i] *Department of Chemical and Geological Sciences, University of Cagliari, Italy*
[j] *Department of Phisics and Earth Sciences, University of Messina, Italy*
[k] *Department of Biological, Geological and Environmental Sciences, University of Catania, Italy*
[l] *CNR, IRPI, Bari, Italy*
[m] *MedSharks, Roma, Italy*
[n] *Department of Biological and Environmental Sciences and Technologies, University of Salento, Lecce, Italy*
[o] *Aix-Marseille Université, CEREGE CNRS-IRD UMR 34, Europole de l'Arbois Aix-en-Provence, France*

ARTICLE INFO

Accepted 20 March 2015

Keywords:
Tidal notches
Mediterranean Sea
Relative sea level rise
Holocene

ABSTRACT

Recent works (Evelpidou et al., 2012) suggest that the modern tidal notch is disappearing worldwide due sea level rise over the last century. In order to assess this hypothesis, we measured modern tidal notches in several of sites along the Mediterranean coasts. We report observations on tidal notches cut along carbonate coasts from 73 sites from Italy, France, Croatia, Montenegro, Greece, Malta and Spain, plus additional observations carried outside the Mediterranean. At each site, we measured notch width and depth, and we described the characteristics of the biological rim at the base of the notch. We correlated these parameters with wave energy, tide gauge datasets and rock lithology.

Our results suggest that, considering 'the development of tidal notches the consequence of midlittoral bioerosion' (as done in Evelpidou et al., 2012) is a simplification that can lead to misleading results, such as stating that notches are disappearing. Important roles in notch formation can be also played by wave action, rate of karst dissolution, salt weathering and wetting and drying cycles. Of course notch formation can be augmented and favoured also by bioerosion which can, in particular cases, be the main process of notch formation and development.

Our dataset shows that notches are carved by an ensemble rather than by a single process, both today and in the past, and that it is difficult, if not impossible, to disentangle them and establish which one is prevailing. We therefore show that tidal notches are still forming, challenging the hypothesis that sea level rise has drowned them.

1. Introduction

Marine tidal notches (hereafter MTNs) are indentations or undercuttings, few centimetres to several metres deep, cut in steep calcareous cliffs at or near sea level (Carobene, 1972; Pirazzoli, 1986; Kelletat, 2005). Although the measurement of tidal notches

* Corresponding author. Department of Earth Sciences, Mineralogy-Geology Edifice (no. 5), Sapienza University, 5 Aldo Moro square, 00185, Roma, Italy.
E-mail address: valeria.lopresti@uniroma1.it (V. Lo Presti).

in the field is trivial and can be done using simple instruments such as a stick metre, two aspects in the study of notches remain challenging. The first is the understanding of the mechanisms of their formation, which can be ascribed to chemical dissolution processes in the intertidal zone, wetting and drying cycles, biological erosion or wave action or, most likely, a combination of these factors. The second is that notches cannot be dated directly, and the estimate of their age relies, in the best cases, on the dating of organisms that form the biological rim covering part of the notch (Pirazzoli et al., 1994; Faivre et al., 2013) or correlating the elevation of a notch with other datable markers. In the worst cases, relative age estimates can be obtained comparing notch (bio)erosion rates and the dimensions of the notch.

Due to the difficulty in establishing the age of MTNs, there is an ongoing debate regarding their origin. The classical view is that MTNs are shaped around mean sea level and each time that a MTN is found out of the tidal range, or each time its shape deviates from the typical half-ellipsoidal shape (Carobene, 1972; Pirazzoli, 1986), there has been either a rapid (coseismic or volcano-tectonic) or a gradual (e.g. due to regional tectonic processes) land movement. To this view, some authors (Cooper et al., 2007; Evelpidou et al., 2012) countered a model where formation of notches can happen only during periods of relative climatic and sea level stability, when bioerosion can 'keep up' with the pace of sea level rise.

Based on areas located in Greece (coasts of the Corinth Gulf, the Euboean Gulf and several Cyclades islands), Evelpidu et al. (2012) stated that: *'The most recent continuous sea level rise has resulted to the absence of a present-day notch*'.

Building on this hypothesis, Pirazzoli and Evelpidou (2013) state that present-day tidal notches are not forming anymore near sea level, while a 'fossil' tidal notch (developed before the sea level rise of 19th and 20th century) is often found between −20 and −65 cm below present sea level. They assert that '*present-day tidal notches are worth being re-measured and re-interpreted*'. One consequence of their hypothesis is that, if proved, tidal notches would lose most of their significance as markers of more or less rapid tectonic movements. Boulton and Stewart (2014) addressed this discussion by analysing a database of Holocene tidal notches dated using radiocarbon ages on fossil incrustation on the notch. They showed that the notches are not clustered around any known period of climatic stability as it would be expected if the hypothesis advanced by Cooper et al. (2007) is valid.

This ongoing debate, coupled to the observation of the presence, along the world's stable sedimentary carbonate coasts, of modern tidal notches, stimulated the collaboration of the group of researchers authoring this paper. We performed a reassessment of notches that are located near present sea level at 73 sites distributed along many carbonate coasts of the Mediterranean Sea (Fig. 1a; S1 supplementary material, hereafter SM). These sites were selected because their relative tectonic stability has been postulated on the basis of independent markers, most often the elevation of the Last Interglacial shoreline (MIS 5e, ~125 Ka ago, Ferranti et al., 2006, and references therein). We collected in-situ observations and measurements of the morphology of MTNs along the coasts of Croatia, France, Greece, Italy, Malta, Montenegro and Spain. In addition, we incorporate observations carried at 5 stable sites outside the Mediterranean Sea.

At each site we measured the different elements of MTNs and the presence, thickness and characteristics of the algal rim, as well as the lithological composition of the limestone. We then compare the measured notches and the thickness of the algal rims to wave energy and tidal ranges, to contribute to the understanding of notch formation. In this paper we show the implications of our results in terms of processes contributing to the shaping of tidal notches and relationship between tidal notches and sea level.

2. Notches in the Mediterranean: relevant aspects

2.1. Geologic context of the Mediterranean basin

The Mediterranean area marks the broad convergent boundary between the African and the Eurasian plates. The geodynamic characteristics of this region are dictated by lithospheric blocks showing different structural and kinematic interaction, including collision, subduction, back-arc spreading, and fold-and-thrust belt development. The complexity of the orogen is attributable in large part to the original geometry of the opposing plate margins and the existence of continental blocks within the western Tethys (Channell and Horvath, 1976; Jolivet and Faccenna, 2000; Serpelloni et al., 2007; Royden and Papanikolaou, 2011, Fig. 1b).

The coasts straddling the Mediterranean orogenic belts are characterized by a variable pattern of long-to short-term vertical tectonic motion, as documented by the elevation of ancient strandlines (Ferranti et al., 2006, 2010). An estimate of the stability of Mediterranean coastal areas can be derived from geomorphological indicators of the Holocene and of the Last Interglacial shoreline position. From these data it is evident that many sectors of the Mediterranean Sea exhibit significant vertical tectonic movements at least since MIS 5.5 and up to the recent (Ferranti et al., 2006, 2010) (Fig. 1c). Conversely, others sectors can be considered stable or affected by very low tectonic motions; these last are the areas studied in this work. Stratigraphic, morphological paleontological, archaeological and chronological data (Flemming and Webb, 1986; Pirazzoli, 1991; Antonioli et al., 2009; Ferranti et al., 2010; Vacchi et al., 2012; Sulli et al., 2013; Anzidei et al., 2011; 2014), indicate that, in general, the western Mediterranean coasts can be considered tectonically stable in the last 125 ka, while large sectors of Italy, Greece and Turkey are characterized by rapid transitions between subsiding, uplifting or stable coasts during the same span of time. On the other hand, stability or low tectonics characterize in general the coasts of North Africa for which published paleo shorelines exist.

2.2. Climate, waves, hydrological conditions and tides

Enclosed between the storm belt of northern Europe and the tropical area of northern Africa, the Mediterranean has a relatively mild climate on the average, but substantial storms are possible, usually in the winter months (Cavaleri et al., 1991; Cavaleri, 2000). The Mediterranean winter climate is dominated by the westward movement of storms originating over the Atlantic and impinging upon the western European coasts, he maximum measured significant wave height reaches 10 m, but model estimates for some non-documented storms suggest larger values (Giorgi and Lionello, 2008). Furthermore, Mediterranean storms can be produced within the region in cyclogenetic areas such as the lee of the Alps, the Gulfs of Lyon and Genoa; moreover, the number of exceptional storms linked to Tropical-Cyclones generated in Southern Mediterranean region is recently increasing (Lionello et al., 2006; Rebora et al., 2013). High pressure and descending motions dominate instead during the summer period, leading to dry conditions particularly in the southern Mediterranean.

The summer Mediterranean climate variability has been found to be connected with both the Asian and African monsoons and with strong geopotential blocking anomalies over central Europe (Alpert et al., 2006; Giorgi et al., 2008). The coasts of Mediterranean Sea are genetically connected to the presence of extended catchments shaped on carbonatic rocks. As such, they are largely characterized by karst groundwater springs, that reach the surface both above or below mean sea level. Such springs have been inferred to influence the development of marine notches (Higgins, 1980;

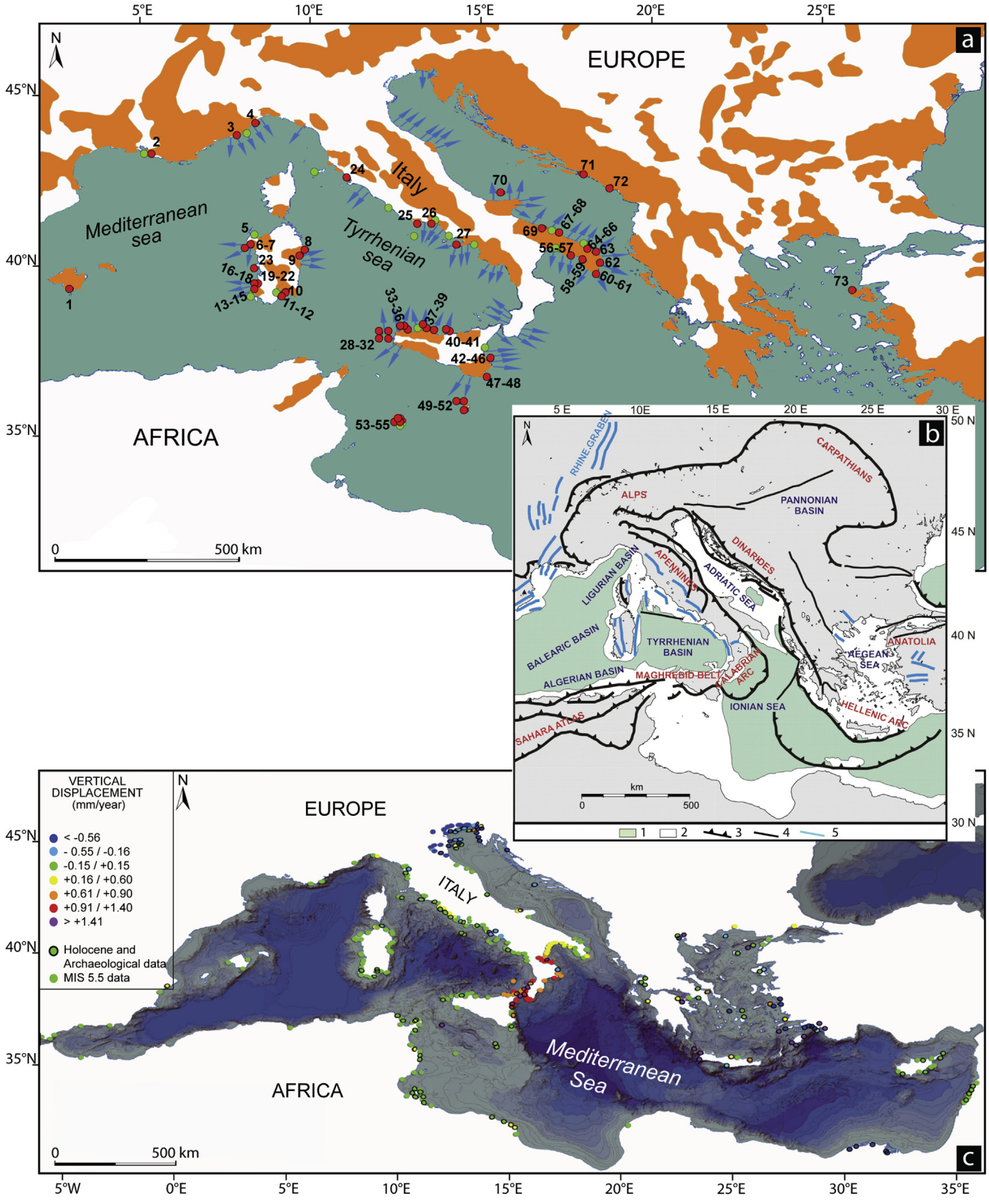

Fig. 1. **a)** Main carbonate outcrops along the Mediterranean coasts (orange); location of studied tidal notches (red dots with numbers, Table 2; S1 SM); location of tide gauges (green dots); coastal and submarine springs with outflows higher than 1000 L per second (blue arrows from Civita, 2008). **b)** Tectonic setting of western and central Mediterranean region (modified after Oldow et al., 2002): 1) Water depth >1000, 2) Water depth 0–1000 m, 3) Contractional fault system, 4) Transcurrent fault systems, 5) Extensional fault system. **c)** Holocene and MIS 5.5 vertical tectonic movements along the Mediterranean coasts. Data calculated from: Antonioli et al., 2009; Faivre et al., 2010, 2011, Ferranti et al., 2006, Ferranti et al., 2010, Galili et al., 2011; Pavlopulos et al., 2012, Radic Rossi and Antonioli 2008, Rodriguez-Vidal et al., 2007; Poulos et al., 2009; Stanley and Toscano 2009; Stewart and Morhange 2009; Tsimplis et al., 2011; Yaltirak et al., 2002; Vött 2007. (For interpretation of the references to colour in this figure legend, the reader is referred to the web version of this article.)

Furlani et al., 2014a). Karst drainage systems can be responsible of high discharges of water, as they represent most often the output point of extensive networks of groundwater conduits. Flows from springs can be perennial, seasonal or intermittent. Most often, in the Mediterranean, their water load follows the seasonal pattern of the rainfall regime. During strong rainfall events, or flash floods due to Cyclonic perturbations, a large number of new springs can be activated (Bonacci et al., 2006). In Fig. 1a we show a map of the coastal and submarine springs with outflow larger than 1000 L per second (Civita, 2008). Although this map is probably biased by a higher concentration of survey in the Italian peninsula, it can give an idea of how widespread are submarine springs along carbonatic coasts. We highlight that the Greek territory is also characterized by a high number of submarine springs (Fleury et al., 2007).

Tides vary from place to place along the coasts of the Mediterranean, depending on many parameters, such as coastal geometry and *bathymetry*, but in general Mediterraenan tides have lower amplitudes with respect to oceanic ones. The average tidal amplitude is about 40 cm, with the exception of exceptional tides observed in the Gulf of Gabes and in parts of the North Adriatic sea, where they may reach amplitudes up to 1.80 m. In other areas, such as in Greece or Sicily, tides are very small, especially near the amphidromic points where the tidal range is almost non-existent. In the vicinity of the Strait of Gibraltar, the Atlantic ocean affects the tides of the Mediterranean, but its influence rapidly declines further east. However, atmospheric conditions may affect the rhythmic tidal rise and fall in sea level, causing larger oscillations or even hide them at all.

2.3. Formation of notches

Nearly half of the Mediterranean rock coasts (Fig. 1a) are built of carbonatic rocks (Furlani et al., 2014b) that date back from Mesozoic to Quaternary. Sedimentary carbonate coasts are characterized by a typical set of landforms (Taborosi and Kazmer, 2013), which are related to a combination of physical, chemical, and biological processes. Their relative importance is dependent on the geographical setting and the local conditions. Chemical solution and biological weathering are the driving factors in sedimentary carbonate coasts development in the Mediterranean coasts (De Waele and Furlani, 2013).

In this study we focus on two coastal landforms, typical of carbonate rocks: marine tidal notches and roof notches. We define Marine Tidal Notches (MTNs) the undercuttings found at or near tidal level on carbonatic cliffs with characteristic shaped morphology (Fig. 2a,b,e). MTNs are characterized by both roof and a floor, which is often covered by biological incrustations. In the particular case where the notch lacks a floor, we defined it as Roof Notch (hereafter RN, Fig. 2c). Hereafter we refer in general to 'notches' to indicate both MTNs and RNs. MTNs and RNs are most common on carbonate rocks, although recently Trenhaile (2014) has argued that notches form also as a consequence of wetting and drying cycles in volcanic lahar deposits in Mexico. Focussing on carbonate rocks, four main processes are considered responsible for the formation of notches: biological agents, wetting and drying cycles and salt weathering, hyperkarst processes and mechanical erosion.

2.3.1. Biological agents

Different kinds of organisms live attached to the rock near sea level. In general, bioeroders contribute to the evolution of notches, while encrusting organisms protect it from deepening. The most known bioeroder in the Mediterranean is *Lithophaga lithophaga*, an endolithic bivalve which lives in galleries bored in calcareous rocks by glandular secretions (Morton and Scott, 1980). Another important class of bioeroders are grazers (mainly sea urchins), that play a major role along coral reef coastlines (Peyrot-Clausade et al., 2000; Spencer and Viles, 2002). In the Mediterranean, Torunski (1979), quantified bioerosion by urchins in 19 g $CaCO^3$ m^{-2} for *Paracentrotus lividus*, and in 295 g $CaCO^3$ m^{-2} for *Sphaerechinus granularis*. In the Mediterranean, *S. Granularis* erosion rates may vary between 16 and 210 g $CaCO^3$ m^{-2} (Sartoretto and Francour, 1997), the higher values corresponding to areas where *S. granularis* is steadily replaced by *Echinus melo*, another large echinoid (Laborel et al., 1961). Lithophaga and echinoids live around mean sea level, therefore they may have a role in shaping the lower part of the notch, which is continuously submerged. Also, when sea level changes, their role remains unchanged. Further bioerosion is caused by endolithic Cyanobacteria (Le Campion-Alsumard, 1979) in the supralittoral zone, together with limpets (*Patella* spp.) and Chitons in the midlittoral zone (Laborel and Laborel-Deguen, 1996).

While bioerosion plays a role in the consummation of rocks in the intertidal zone, some hard bottom communities can protect the bedrock from erosion (Laborel and Laborel-Deguen, 1996; Naylor and Viles, 2002; Spencer and Viles, 2002). In the Mediterranean, constructional (and therefore protective) elements are the rim-building coralline rhodophyte *Lithophyllum lichenoides*, brown algae (*Cystoseira* and *Sargassum*), fixed Vermetid Gastropod Molluscs (*Dendropoma* spp., *Petaloconchus* spp.), Cirrhipeds (*Balanus* sp. and *Tetraclita* spp), as well as *Mytilus* sp. and *Ostrea* sp.

2.3.2. Wetting and drying cycles and salt weathering

The importance of these processes in notch formation has been recently highlighted by Trenhaile (2014). In the spray zone, called supralittoral in biological zonation (Laborel and Laborel-Denguen, 1996), haloclastic processes trigger cliff erosion through the penetration of saline water into structural discontinuities of the bedrock and its evaporation, with the subsequent deposition of salt crystals, which can grow from solution, expand due to heating or change their volume due to hydratation. These processes lead to modification in the volume of the crystals, which causes an increase of pressure on the walls, triggering the fragmentation of the rock. Another important weathering process along rocky coastlines is associated to wetting and drying cycles (Stephenson and Kirk, 2000; Kanyaya and Trenhaile, 2005; Trenhaile and Porter, 2007). In cold climates, weathering due to frost action plays also a significant role in the upper part of the cliff (Trenhaile and Mercan, 1984).

2.3.3. Hyperkarst

The debate upon the possibility that limestones can be dissolved in seawater lasts since the early 30's (MacFadyen, 1930). Solution of a calcareous rock depends on the saturation of the seawater with respect to calcium carbonate. If the seawater is under saturated in this component with respect to the lithology, then dissolution can occur. This happens in proximity of springs of groundwater (Higgins, 1980) or due to water mixing (Kaye, 1957; Verstappen, 1960) or by surface film effects due to gaseous exchanges with the air (Emery, 1962). Kelletat, 2005, argues that seawater is always oversaturated (in tropical and subtropical latitudes several times supersaturated) by dissolved carbonates and is not able to destroy carbonates by solution. To falsify this hypothesis, Furlani and Cucchi, 2013 collected micro erosion metre data on a vertical limestone slab in the Adriatic Sea and suggested that the shape of the tidal notch is consistent with the distribution of erosion rates along the slab.

2.3.4. Mechanical erosion

While wave abrasion *sensu stricto* (i.e. wave abrasion due to sand or pebbles used as abrasion tools against the rock) plays no part in the development of a tidal notch, mechanical erosion can still

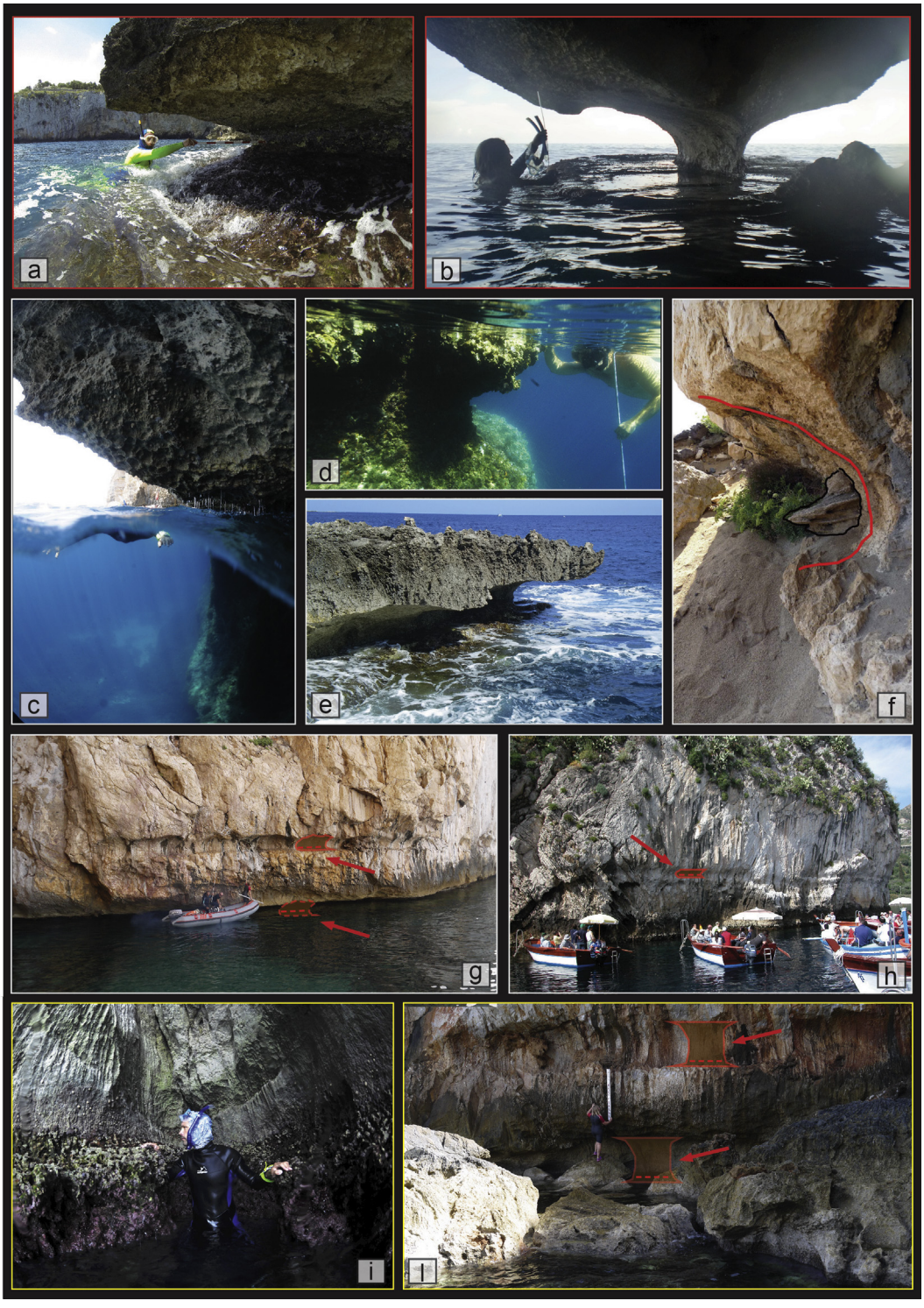

Fig. 2. Notches along the central Mediterranean carbonatic coast: **a)** a tidal notch (Zinzulusa, Apulia). **b)** an impressive tidal notch on an isolated limestone rock (Cala Fuili, Sardinia). **c)** a roof notch (Malta) **d)** a submerged notch (Limski canal, Croatia). **e)** a well developed tidal notch carved on the rocky headlands of Favignana. **f)** Eolianite deposit covering the Last Interglacial notch (Biddiriscottai, Sardinia), **g)** Modern and MIS 5.5 tidal notches (Masua, Sardinia), **h)** uplifted tidal notch (Taormina, Sicily), **i)** one metre high corallinae algae in a cul de sac with high pressure splash (Malta) **I)** outsized notch in a cul de Sac (Buggerru, Sardinia).

happen in the intertidal to slightly supratidal zone – in function o f the deep at the base of the cliff and relatively to the impacting wave features – for two main reasons. First, the resistance of the rock to wave attack is function of its lithology and of the structural discontinuities characterizing it (Kleypas et al., 1999). These can be cracks, cleavages, joints, faults, and bedding planes, some being inherent in lithology and others being of tectonic origin. Under wave action, the air contained inside the interstices is suddenly compressed, resulting in a pressure increase exerting a stress on the walls of the opening, widening and deepening it until the removal of part of the rock. This process acts in the zone where air and water alternate, i.e. above and below the fluctuating waterline (Trenhaile,

2002). Second, along limestone coastlines, chemical and biochemical dissolution processes happening near tidal level may favour mechanical erosion by influencing the material properties of rock, and weakening or creating joint or boundaries (for details, see Table 4 of Naylor et al., 2012).

2.4. Rates of erosion in the intertidal zone

What are the rates at which tidal notches are forming? Field measurements of erosion rates in the intertidal zone have been conducted in different areas since the end of the seventies mainly using Micro Erosion Meters (MEM) and Traversing Micro Erosion Meters (TMEM), mostly on shore platforms and sloping limestone surfaces (Furlani and Cucchi, 2013). Torunski (1979) reported erosion rates in the range of 0.07–1.114 mm/yr from a carbonate intertidal zone of the northeastern Adriatic, which is mainly composed by low-angle plunging cliffs. Furlani et al. (2009) indicated lower values for the supratidal zone (0.09–0.194 mm/yr), and suggested that erosion rates in the supratidal and subtidal zone are one order of magnitude lower than the intertidal zone for the same type of coast. It has been pointed out that seasonal variations are possible in carbonate lowering rates, with higher rates in summer (Torunski, 1979) and in autumn (Furlani et al., 2009). A compilation of coastal erosion rates, derived and adapted from Furlani et al., 2010, is presented in the supplementary material (S2 in SM) attached to this publication.

In some cases, such as in the Gulf of Trieste, the lack of the present-day notch and the occurrence of an underwater notch (Fig. 2d) has been related either to the tectonic subsidence of the area (Antonioli et al., 2004, 2007) or to temperature variations, such as the Medieval Warm Period where enhanced dissolution was possible. In the Gulf of Trieste, Furlani et al. (2010) estimated erosion rates of limestone surfaces located in the intertidal zone, and on the contribution of seawater and the bioerosion effects to notch development (Furlani and Cucchi, 2013), using a MEM. Furlani and Cucchi (2013) measured maximum rates up to about 0.3 mm/yr occurring in the mid-intertidal zone. Overall, measurements indicate that lowering rates (that include all the notch formation processes) range from 0.02 to 2.1 mm/yr, a range which contains the rates of bioerosion reported by Evelpidou et al., 2012 of 0.2–1.28 mm/yr.

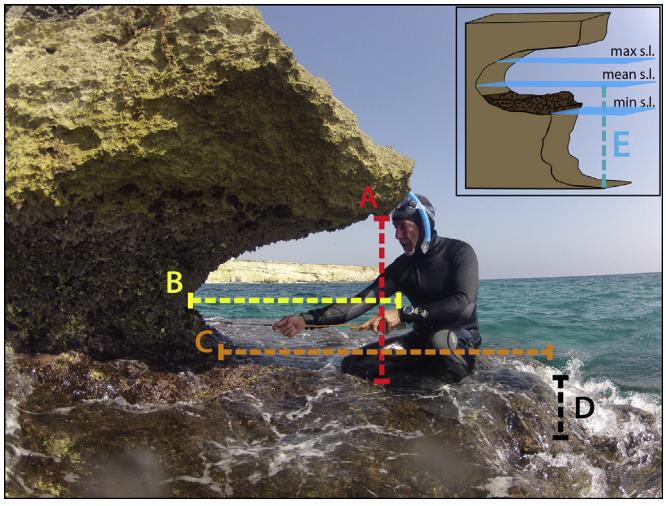

Fig. 3. Morphometric measures: A) Average notch width, B) Notch depth, C) Bottom depth (reef when present), D) reef and step (if present) thickness, E) Depth of cliff toe at mean sea level.

3. Methods

3.1. Field observations

In this study, we report the results of the survey of the modern notch in 71 out of 73 visited sites along carbonate coastlines in the Mediterranean.

A standardized terminology defining the morphological features of the notches is not available in literature, and often the same measure is reported with different names. To clarify our terminology, we report a graphic view of it in Fig. 3. During our field

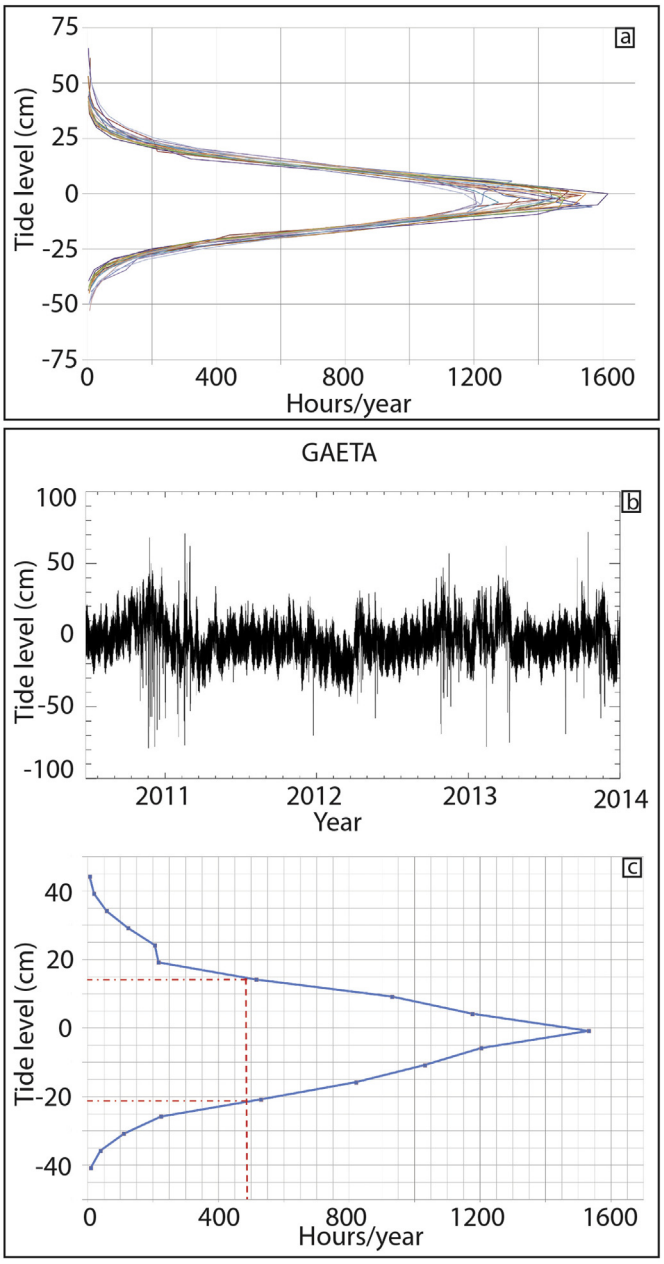

Fig. 4. Statistical diagrams of tide gauges data: **a)** height tide trend (hours/year) of the analysed tide gauges: Bari, Naples, Ponza, Catania, Marseille, Elba; Civitavecchia, Gaeta, Carloforte, Cagliari, Imperia, Otranto, Lampedusa, Palermo, Porto Torres, Taranto; **b)** Gaeta tide gauge: tide trend from 2010 to 2014; **c)** Gaeta tide gauge: trend of tide (hours/year, blue line); mean value of significant height tide (vertical axis) and significant hours/year at the same height tide, horizontal axis. (For interpretation of the references to colour in this figure legend, the reader is referred to the web version of this article)

Table 1
Data obtained from tide gauges (Fig. 4 for example) and the OSU tidal prediction model, regional solution for the Mediterranean. **1** Station names. **2** lower L_{min} and upper L_{max} values of the residual sea level calculated for about 10 h/year. **3** Sum of values on column 2: maximum tide level. **4** Number of hours for year at the histogram maximum (Fig 4), tide level values at half maximum of the histogram (sixth and seventh columns). **5**–**6** Lower and upper limit at half maximum (cm) of the histogram. **7** Sum of columns 5 and 6. **8** Average notch width cm (see Table 2).We show that overall, the root mean square error between the tidal gauge data and the model data is ~4 cm.

1	2		3	4	5	6		7	8
Tide gaudge station[1]	L_{min} (cm)[2]	L_{max} (cm)	Maximum tidal level	Maximum value of hours/year	Significant hours	Lower and upper value at significant hours (cm)		Mean tide value at half maximum tide level (cm)	Values obtained from OSU tidal model (cm)
Bari	−44.9	55.1	99	1223.38	586.75	−19.9	15.1	35	37.7
Cagliari	−41.2	38.8	80	1510.32	711.05	−16.2	13.8	30	27.9
Palermo	−52.8	42.2	95	1410.15	543.8	−17.8	17.2	35	34.5
Civitavecchia	−41.9	43.1	85	1343.29	549.25	−21.8	13.2	35	–
Carloforte	−38.7	51.3	90	1494.60	588.1	−18.7	11.3	30	28.4
Catania	−40.0	35.0	75	1616.03	617.45	−15.1	14.9	30	23.8
Elba	−40.9	44.1	85	1566.48	647.15	−15.9	14.1	30	32.4
Imperia	−42.1	37.9	80	1481.72	629.8	−17.1	12.9	30	31.2
Lampedusa	−42.2	37.8	80	1442.68	614.15	−17.2	12.8	30	25.6
Marseille	−39.3	55.7	95	1527.65	647.6	−19.3	10.7	30	27.8
Napoli	−43.9	41.1	85	1275.24	563.2	−18.9	16.1	30	38.2
Otranto	−40.0	40.0	80	1547.23	455.6	−20.0	15.0	35	25.8
Ponza	−44.3	35.7	80	1317.40	533.75	−19.2	15.7	35	37.9
Porto Torres	−43.2	36.8	80	1475.44	480.7	−18.2	16.8	35	27.9
Salerno	−49.5	45.5	95	1207.8	439.75	−19.5	20.5	40	38.2
Taranto	−42.2	42.8	85	1461.16	643.35	−17.2	12.8	30	22.1
Gaeta	−40.8	44.2	85	1532.25	485.9	−20.8	14.2	35	37.9
								RMSE	**4.08**

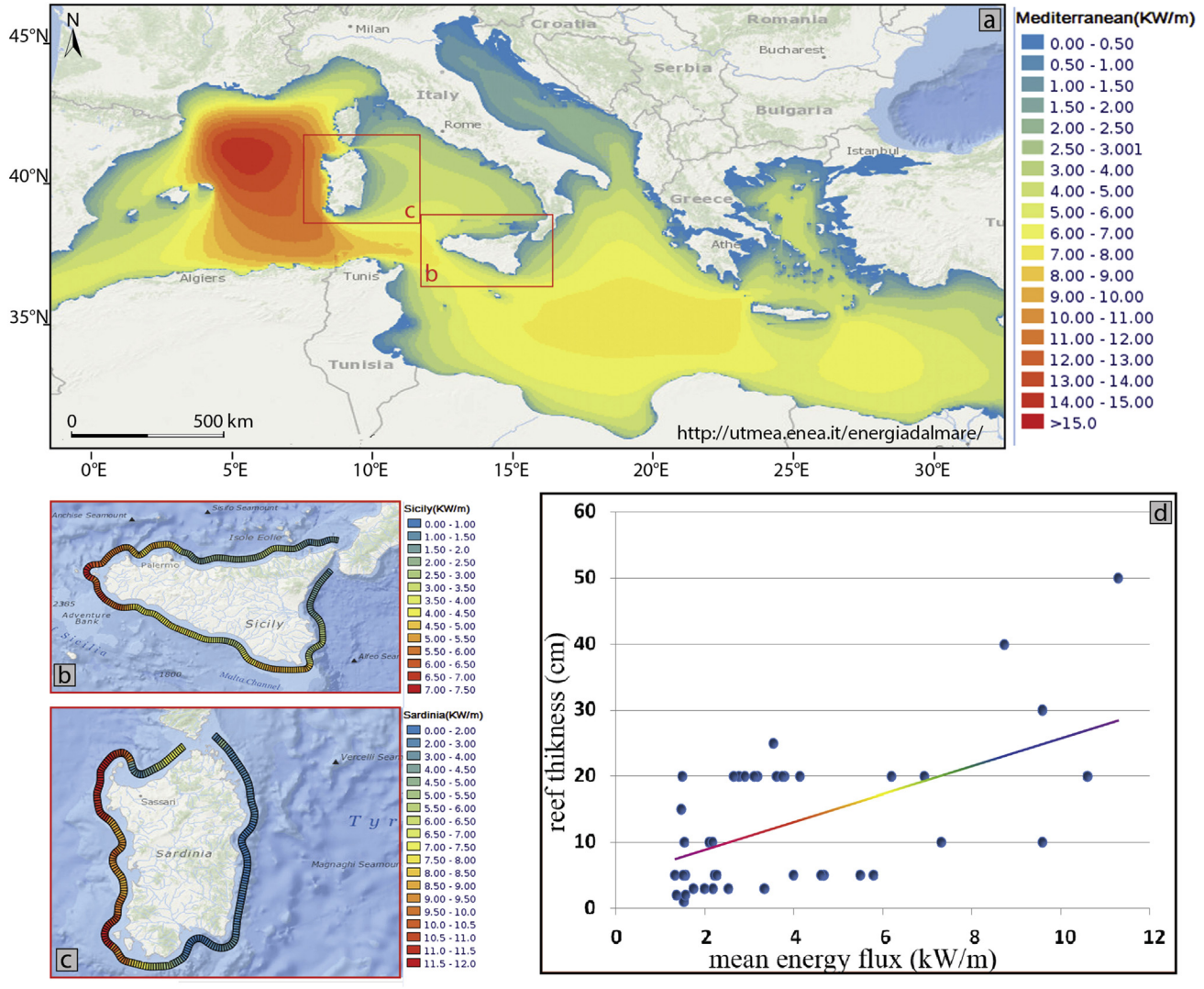

Fig. 5. Mediterranean mean waves Energy Flux (kW/m) http://utmea.enea.it/energiadalmare/ (**a**). Zoom of mean waves energy flux in Sardinia and Sicily (**b and c**). Correlation between the rim thickness and mean waves energy flux (**d**).

Table 2
Tidal notches data in Mediterranean Sea **1)** Site number; **2)** Site name; **3)** Type of notch; **4)** Average notch with; **5)** Average notch depth; **6)** Bottom depth of biological rim; **7)** Thickness of biological rim; **8)** Tidal range as predicted by OSU model; **9)** Width of MIS 5.5 notch (if present); **10)** Exposure.

Site N	Site name	Type of notch	Average notch width with uncertainty (cm)	Average notch depth with uncertainty (cm)	Thickness of biological rim with uncertainty (cm)	Tidal range as predicted by OSU model (cm)	MIS 5.5 notch width (cm)	Exposure
1	Colonia de S.Jordie Palma	MTN	55 ± 2.8	90 ± 4.5	2.5 ± 0.1	18.7	–	Exp.
2	Marseille Fausse Monnaie	RN	30 ± 1.5	50 ± 2.5	2.5 ± 0.1	27.8	–	Exp.
3	Balzi Rossi Ventimiglia	MTN	44 ± 2.2	60 ± 10.4	10 ± 0.5	30.5	–	Exp.
4	Noli Malpasso	MTN	100 ± 5	75 ± 25.3	1 ± 0.1	31.2	–	Exp.
5	Capo Caccia	MTN	70 ± 3.5	80 ± 63.1	45 ± 2.3	27.9	0.75	Exp.
6	Porto Conte	MTN	48 ± 2.4	30 ± 1.5	5 ± 0.3	25.8	0.70	Shelt.
7	Porto Conte	MTN	60 ± 3	60 ± 3	10 ± 0.5	23.6	0.70	Shelt.
8	Biddiriscottai	MTN	60 ± 5	70 ± 3.5	10 ± 0.5	34.1	0.80	Shelt.
9	Cala Fuili	MTN	70 ± 4.9	80 ± 160	10 ± 0.5	32.6	0.75	Exp.
10	Sella del Diavolo	MTN	55 ± 2.8	100 ± 5	15 ± 0.8	25.0	–	Exp.
11	Cala Mosca	MTN	50 ± 2.5	190 ± 41.1	15 ± 0.8	27.9	–	Exp.
12	Cala Mosca	MTN	55 ± 2.8	175 ± 26.5	15 ± 0.8	27.3	–	Exp.
13	Masua	MTN	50 ± 2.5	75 ± 6.3	10 ± 0.5	24.5	0.75	Exp.
14	Masua	MTN	60 ± 4.6	140 ± 7	20 ± 1	27.2	–	Exp.
15	Masua	MTN	48 ± 2.4	50 ± 2.5	20 ± 1	28.4	–	Exp.
16	Pan di zucchero	RN	30 ± 1.5	30 ± 1.5	20 ± 1	28.3	–	Exp.
17	Pan di zucchero	MTN	66 ± 3.3	120 ± 20.9	15 ± 0.8	26.7	–	Exp.
18	Pan di zucchero	MTN	50 ± 2.5	60 ± 3	20 ± 1	24.2	–	Exp.
19	Cala Domestica	MTN	48 ± 2.4	50 ± 2.5	5 ± 0.3	28.1	–	Exp.
20	Cala Domestica	MTN	78 ± 3.9	60 ± 3	10 ± 0.5	26.3	–	Exp.
21	Buggerru	MTN	68 ± 3.4	60 ± 3	10 ± 0.5	22.9	–	Exp.
22	Buggerru	MTN	73 ± 3.7	80 ± 4	30 ± 1.5	25.3	0.8	Shelt.
23	Tharros	MTN	72 ± 3.6	60 ± 3	3 ± 0.2	28.9	–	Exp.
24	Talamone	MTN	42 ± 2.1	40 ± 2	2 ± 0.1	32.4	–	Exp.
25	Circeo	No Notch	–	–	15 ± 0.8	36.9	0.26	Exp.
26	Gaeta	MTN	35 ± 1.8	40 ± 2	35 ± 1.8	37.9	0.50	Exp.
27	Capri	No Notch	70 ± 3.5	40 ± 2	15 ± 0.8	38.2	0.70	Exp.
28	Marettimo Harbour	MTN	55 ± 2.8	100 ± 5	5 ± 0.3	26.4	–	Shelt.
29	Marettimo Castello	MTN	60 ± 3	70 ± 3.5	10 ± 0.5	26.8	0.75	Exp.
30	Favignana Cala rossa	MTN	60 ± 3	70 ± 75.1	20 ± 1	27.2	–	Exp.
31	Levanzo	MTN	60 ± 3	40 ± 2	15 ± 0.8	32.0	–	Exp.
32	Levanzo Harbour	MTN	60 ± 3	100 ± 5	15 ± 0.8	29.6	–	Exp.
33	San Vito Castelluzzo	MTN	52 ± 2.6	40 ± 2	5 ± 0.3	35.9	–	Exp.
34	Macari	MTN	55 ± 2.8	45 ± 2.3	5 ± 0.3	35.9	–	Shelt.
35	Zingaro	MTN	50 ± 2.5	200 ± 10	5 ± 0.3	34.7	–	Exp.
36	Scopello	MTN	50 ± 2.5	60 ± 3	5 ± 0.3	32.3	–	Shelt.
37	Palermo Mondello	MTN	60 ± 3	90 ± 4.5	5 ± 0.3	36.4	–	Exp.
38	Palermo harbour	MTN	55 ± 4.5	70 ± 55.1	5 ± 0.3	34.5	–	Exp.
39	Mongerbino	MTN	70 ± 3.5	85 ± 15.6	5 ± 0.3	37.4	0.80	Exp.
40	Cefalù	MTN	70 ± 3.5	125 ± 25.8	5 ± 0.3	37.7	–	Exp.
41	Cefalù	MTN	60 ± 3	80 ± 4	5 ± 0.3	37.7	–	Exp.
42	Siracusa	MTN	60 ± 3	60 ± 3	20 ± 1	23.8	–	Exp.
43	Siracusa	MTN	45 ± 2.3	60 ± 3	20 ± 1	23.8	–	Exp.
44	Siracusa	MTN	60 ± 3	80 ± 4	20 ± 1	23.8	–	Exp.
45	Siracusa	MTN	30 ± 1.5	70 ± 3.5	20 ± 1	23.8	–	Exp.
46	Siracusa	MTN	62 ± 3.1	150 ± 7.5	20 ± 1	23.8	–	Exp.
47	Marzamemi	MTN	55 ± 2.8	80 ± 4	20 ± 1	24.4	–	Exp.
48	Calamosche	MTN	60 ± 3	80 ± 4	20 ± 1	23.9	–	Exp.
49	Gozo	MTN	95 ± 4.8	80 ± 4	5 ± 0.3	21.4	–	Exp.
50	Gozo Eroded mushroom	MTN	70 ± 3.5	90 ± 4.5	5 ± 0.3	21.0	–	Exp.
51	Comino	MTN	60 ± 3	75 ± 3.8	10 ± 0.5	22.4	–	Exp.
52	Malta	MTN	38 ± 1.9	10 ± 0.5	0 ± 0	25.1	–	Exp.
53	Lampedusa Cala Calandra	MTN	35 ± 1.8	50 ± 2.5	0 ± 0	25.6	–	Exp.
54	Lampedusa	MTN	44 ± 2.2	60 ± 3	3 ± 0.2	24.1	–	Exp.
55	Lampedusa	MTN	36 ± 1.8	40 ± 2	3 ± 0.2	25.2	–	Shelt.
56	Marina di Pulsano	MTN	70 ± 3.5	55 ± 2.8	3 ± 0.2	22.1	–	Shelt.
57	Torre Colimena	MTN	60 ± 3	50 ± 2.5	3 ± 0.2	23.2	–	Exp.
58	Serra Cicora	MTN	45 ± 2.3	130 ± 6.5	10 ± 0.5	22.6	–	Exp.
59	Serra Cicora	MTN	45 ± 2.3	174 ± 8.7	10 ± 0.5	23.3	–	Exp.
60	Santa Maria di Leuca	MTN	60 ± 3	150 ± 7.5	20 ± 1	22.4	–	Exp.
61	Santa Maria di Leuca	MTN	80 ± 4	90 ± 4.5	20 ± 1	21.6	–	Exp.
62	Ciolo	MTN	60 ± 3	90 ± 4.5	20 ± 1	24.9	–	Exp.
63	Zinzulusa	MTN	70 ± 3.5	90 ± 4.5	25 ± 1.3	25.0	–	Exp.
64	Badisco	RN	13 ± 0.7	49.5 ± 8.9	0 ± 0	25.8	–	Shelt.
65	Badisco	MTN	50 ± 2.5	30 ± 1.5	5 ± 0.3	25.8	–	Exp.
66	Badisco	MTN	65 ± 3.3	110 ± 5.5	20 ± 1	25.0	–	Exp.
67	Polignano Modugno	MTN	60 ± 3	30 ± 1.5	40 ± 2	33.3	–	Exp.
68	Polignano San Vito	MTN	70 ± 3.5	90 ± 4.5	2 ± 0.1	36.7	–	Shelt.

(*continued on next page*)

Table 2 (*continued*)

Site N	Site name	Type of notch	Average notch width with uncertainty (cm)	Average notch depth with uncertainty (cm)	Thickness of biological rim with uncertainty (cm)	Tidal range as predicted by OSU model (cm)	MIS 5.5 notch width (cm)	Exposure
69	Giovinazzo	MTN	45 ± 2.3	50 ± 2.5	5 ± 0.3	37.7	–	Exp.
70	Tremiti	MTN	40 ± 2	40 ± 2	0 ± 0	32.1	–	Exp.
71	Dubrovnik	RN	10 ± 0.5	50 ± 2.5	0 ± 0	39.8	–	Shelt.
72	Montenegro	RN	10 ± 0.5	50 ± 2.5	0 ± 0	35.8	–	Exp.
73	Gavathas	MTN	52 ± 2.6	45 ± 10.3	3 ± 0.2	22.6	–	Shelt.

surveys, we took the following measures: i) the average notch width (A) is the average vertical extent of the notch; ii) inward notch depth (B) is the horizontal extent of the notch; iii) inward bottom depth (C) is the horizontal extent of the notch base (when present, corresponding to the biological rim extent); iv) thickness and main species of the biological rim at the notch base (D, when present); v) Depth of the cliff toe (E).

We measured the dimensions of notches with an invar rod, while the geographic positioning was taken with a GPS Garmin Montana 650T and plotted on Google Earth maps (S1 in SM). All coordinates are expressed as Lat/Long in WGS84 reference system. Accuracy of location is within 10 m. All measurements were taken with calm sea and were referred to mean sea level using the tide gauge data from the nearest tidal stations (www.idromare.it; http://www.ioc-sealevelmonitoring.org/map.php), including corrections for atmospheric pressure at the time of measurement. Repeating our measures several time at the same site, we estimated an error of 5% (1 σ) in the recorded values. All our field observations are included as supplementary material to this paper.

We documented individual notches with photographs and videos. Part of this documentation is attached as supplementary material to this publication. At each site we also reported bedrock lithology and age from state geological maps. Finally, we reported the elevation above sea level and width of the Last Interglacial notch, when present. These notches have been preserved in most cases thanks to the presence of younger sediments covering them. In addition to tidal notches in the Mediterranean, we also report the measures of 5 notches outside Mediterranean (see Chapter 5.5), done with the same survey techniques described above.

Supplementary video related to this article can be found at http://dx.doi.org/10.1016/j.quascirev.2015.03.016.

3.2. Tidal ranges

As the availability of tidal records does not cover adequately our measurement sites, we adopted a twofold strategy to include for each observation an estimate of the tidal range. We first analysed the sea level records at 17 stations in the Mediterranean Sea, taken with a sampling rate of one hour. Most data cover about 15 years (Bari, Cagliari, Civitavecchia, Imperia, Marseille, Napoli, Otranto, Palermo, TarantoCarloforte, Catania, Lampedusa, Porto Torres, Salerno). Other tidal datasets span only about 3 years (Gaeta, Ponza and Elba islands). Data from Italian stations have been provided by the Italian tidal network managed by ISPRA (www.mareografico.it); the Marseille record has been retrieved from the Réseaux de réféence des observations marégraphiques (REFMAR, http://refmar.shom.fr/home).

To characterize the sea level variability at each station we show the histogram representing the number of hours per year for which a given sea level occurs (Fig. 4). These plots have been built by calculating the residual sea level (LR) obtained by subtracting the temporal mean <L> from the original sea level time series L:

$$LR = L - <L>$$

Then, the interval over which the residual sea level ranges [L_{min}, L_{max}] is divided into N bins of 5 cm length; the number N depending on the station. N, L_{min}, L_{max} values for each station are shown in Table 1. Finally, the number of data points falling into each bin is counted and converted into hours per year.

As the tide gauge stations often were not close to our study sites, we extracted the tidal ranges for all our 73 locations from the Mediterranean regional version of the Tidal Prediction Software developed at the Oregon State University (OTIS, Gary et al., 2002). The model can be considered as a state-of-art tidal model that assimilates most of the available satellite altimetric data (Topex Poseidon, Topex Tandem, ERS) and in situ observations (i.e. tide gauges, ship born ADCP). The Mediterranean model has a resolution of 1/30° (about 3.7 Km) and makes use of the GEBCO 1′ database as bathymetry. The model considers the main eight tidal components (m2, s2, n2, k2, k1, o1, p1, q1) that account for more than 99% of the total tidal elevation. In Table 1 we report the values calculated using the model described above at our tide gauges against the values calculated from the tide stations. We obtain differences in the range of ~4 cm (Table 1). We highlight that this number should be taken at face value, as it is possible that some of the data in the tide gauges have been used to develop the tidal model, therefore elements of circularity might be present in our calculations. Nevertheless, we argue that the model produces values of tidal range that are consistent with the tide gauge data available.

3.3. Exposure to waves and wave energy

For each site, we used official nautical cartographies and data from oceanographic buoys (http://utmea.enea.it/energiadalmare/) to classify the investigated sites in exposed or sheltered. The yearly climatological wave energy flux (in kW/m) associated to our sites (excluding those with roof notches and those repaired in bays or gulfs) has been estimated using the daily data produced by Liberti et al. (2013) for the period 2001–2010. The computed yearly values are shown in Fig. 5a,b,c.

4. Results

4.1. Notch parameters and bedrock lithology

In this study, we measured the modern notch in 71 out of 73 visited sites along carbonate coastlines in the Mediterranean, as illustrated in Fig. 3 (see also S3). Only at two sites, Circeo and Capri, the notch is absent. The results of our surveys are shown in Table 2, Fig. 6, and contained in full in the supplementary materials (S4). Photographs that illustrate some of the notches are shown in Fig. 2. In average, all the tidal notches we measured are 45–70 cm wide and 40–100 cm deep, although more extreme values are possible.

At all sites, some kind of biological coverage of the notch bottom was found; in this paper we call it 'biological rim', derived from the term 'algal rim' that has been largely used in Mediterranean marine ecology to indicate the rim formed around sea level by corallinaceous algae (Laborel and Laborel-Deguen, 1996). The most

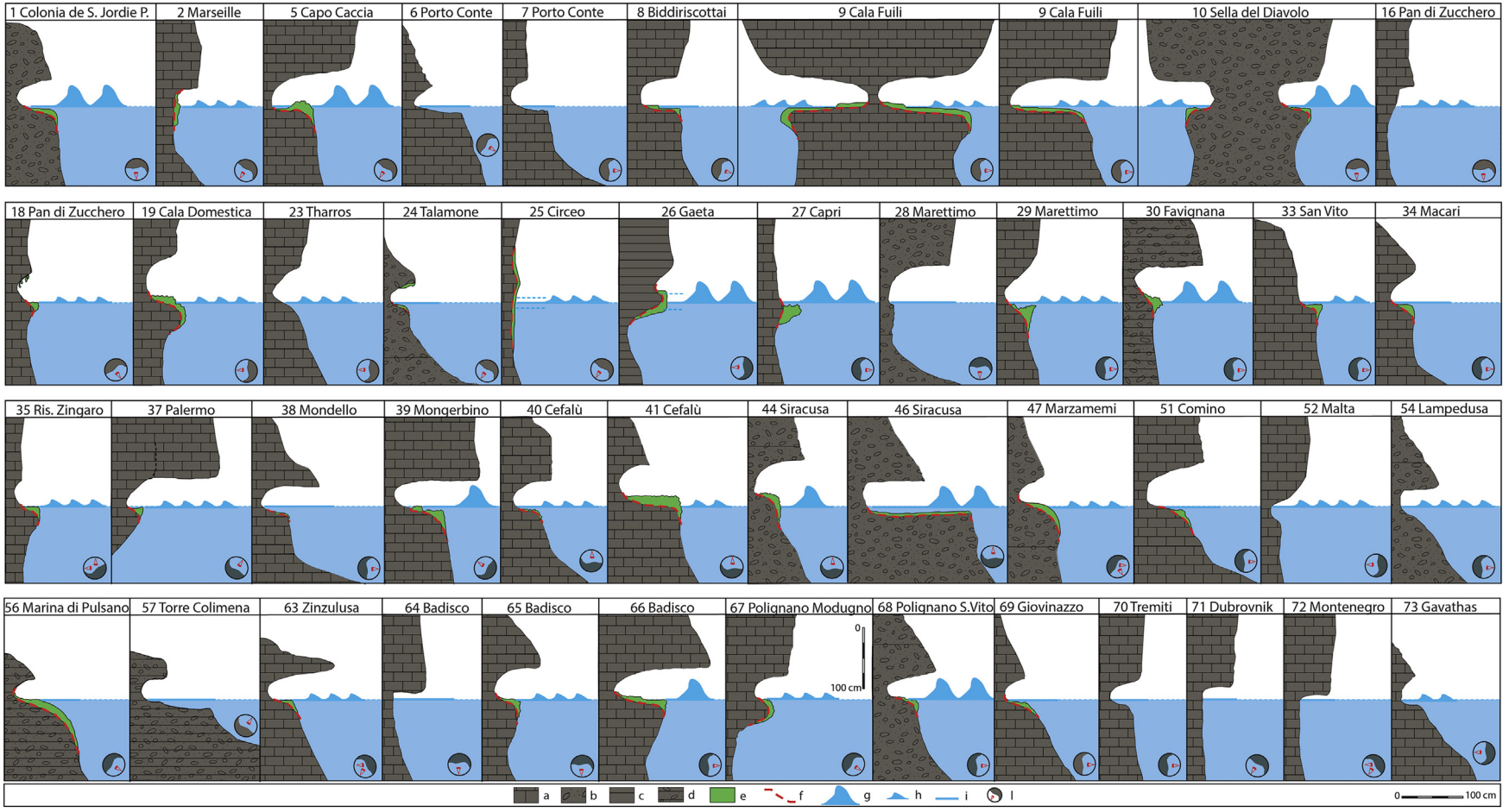

Fig. 6. Representative sections of most significant tidal notches studied. a) limestone, b) sandstone and very erosive limestone, c) stratified limestone, d) stratified sandstone and very erosive limestone, e) reef, f) supposed limit between rock and reef. Fetch and kind of sea energy: g) very exposed, h) exposed, i) sheltered. l) geographical exposure (see Table 2).

Table 3
Geomechanical properties of the rock masses carved by tidal notches.

	Massive limestones	Organogenic limestones	Calcitic dolostones	Dolostones	Calcerenites (sandstones)
Specific Gravity (Gs)	2.65 ÷ 2.73	2.65 ÷ 2.73	2.65 ÷ 2.73	2.65 ÷ 2.73	2.68 ÷ 2.73
Porosity (n%)	4 ÷ 10	10 ÷ 20	10 ÷ 20	4 ÷ 11	44.00 ÷ 50.00
Dry density γd (KN/m^3)					12.4 ÷ 15.20
Water absorption (wa %)	2.00	10.00	10.00	4.00	28.40 ÷ 36.20
Uniaxial Compressive Strenght (MPa)	227.51	135.33	131.40	117.67	2.22 ÷ 5.08
Flexural Strengths (MPa)	20.10	16.67	14.51	11.76	1.09 ÷ 8.10

conspicuous coverage is in fact constituted by corallinaceous algae, especially *Lithophyllum* spp., and Vermetids, but in many cases the biological community inhabiting the notch was composed by Mytilus, Patellae, Chtamalidae and Balanidae. The biological coverage reaches thicknesses of up to 25 cm.

In general, lithology and relative age of geological units on which notches are carved are different (Fig. 6). As highlighted in Table 3 (see also S5), lithologies in our study area range from Early Cambrian dolomites (Gonnesa Formation) in Sardinia to the Middle Trias (Dolomites of San Pietro dei Monti) in Liguria; from Lower Jurassic – Lias (Inici Formation) at Scopello in Sicily, to Upper Jurassic – Malm (Monte Bardia Formation) at Orosei Gulf and Cefalù Formation in Sicily; from the Cretaceous limestone in Apulia to the Oligocene at Talamone (Brecciole Nummulitiche) and in Apulia (Castro Limestone); from the Miocene (Capraia Formation) at the Tremiti Islands to the Miocene–Pleistocene calcarenites at Favignana island and Jonian Apulia.

As a consequence of the great variability in age, lithology, and development of tectonic, the physic-mechanical characteristics of these rocks are quite different. A broad classification is here done between massive (hard rocks) and calcarenites (that can be defined as “weak rocks”).

4.2. Quantitative relation between notch size, tidal and wave conditions, and bedrock lithology

Comparison of the width of notches located near the tide gauge stations with the tidal data (Fig. 7) highlights that the width of the notch is always higher than the mean tidal range, but smaller than the maximum and minimum tidal ranges. In order to investigate how width and depth of notches vary between exposed and sheltered sites, we plotted these values against the tidal range calculated using the OSU tidal model described above (Fig. 8a,b,c,d).

In sheltered areas, the notch width is ~0.3–3.2 times the tidal range (Figs. 8c and 7), a ratio that seems maintained in exposed sites (Fig. 8d,e,f), although with larger variability. In exposed sites, the depth of the notch increases with respect to sheltered sites (Fig. 8a,b). This is also evident by comparing notch width and depth. These results highlight that increased wave action results in an increased notch depth rather than an increased notch width, which seems more constant and related, to some extent, to the tidal range and maximum and minimum tidal values (Fig. 7) (Fig. 8c, d, Table 2, S3 SM). We also highlight that the mean tide never exceeds the maximum notch width (Fig. 7). By grouping our data according to lithology, sandstones and stratified limestone have, predictably, a width/depth ratio lower than massive carbonate rocks (Fig. 8g). This relation supports the notion that in weaker lithologies wave action affects notch depth rather than notch width.

Observations of extra-Mediterranean notches seem to fit these quantitative measures. Notches in Barbados, Zanzibar (Tanzania), Bonaire (Netherland Antilles), Phi Phi island (Thailand), Blue Bay and Port Luis (Mauritius) (Fig. 9, Table 4) show that the present notch is always wider than the maximum local tide.

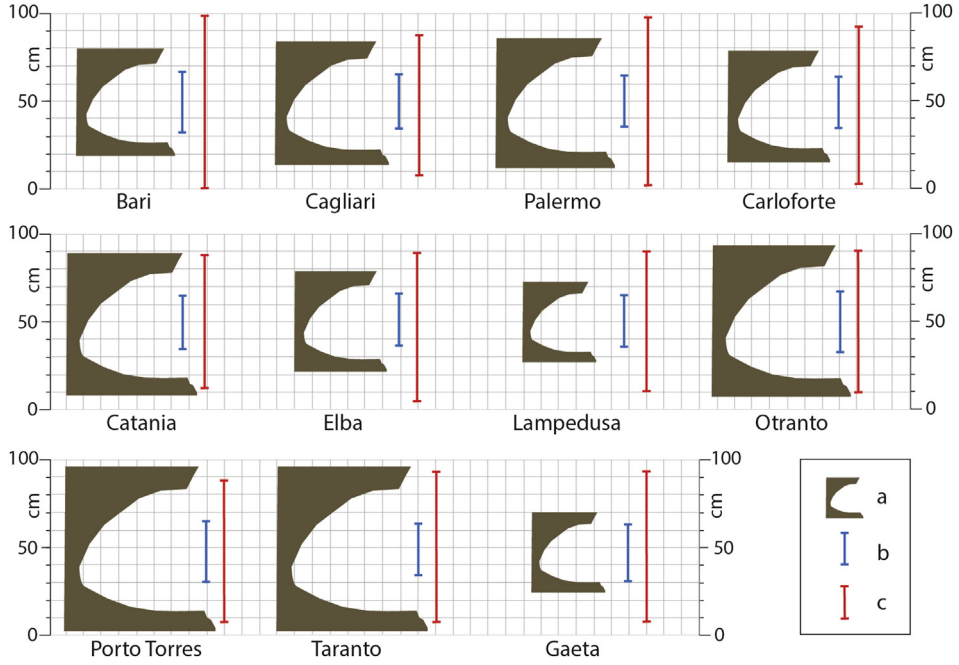

Fig. 7. Relationship between notch width (a), mean tide values (b) and extreme (max–min) tide values (c) in locations where notches have been measured near a tide station.

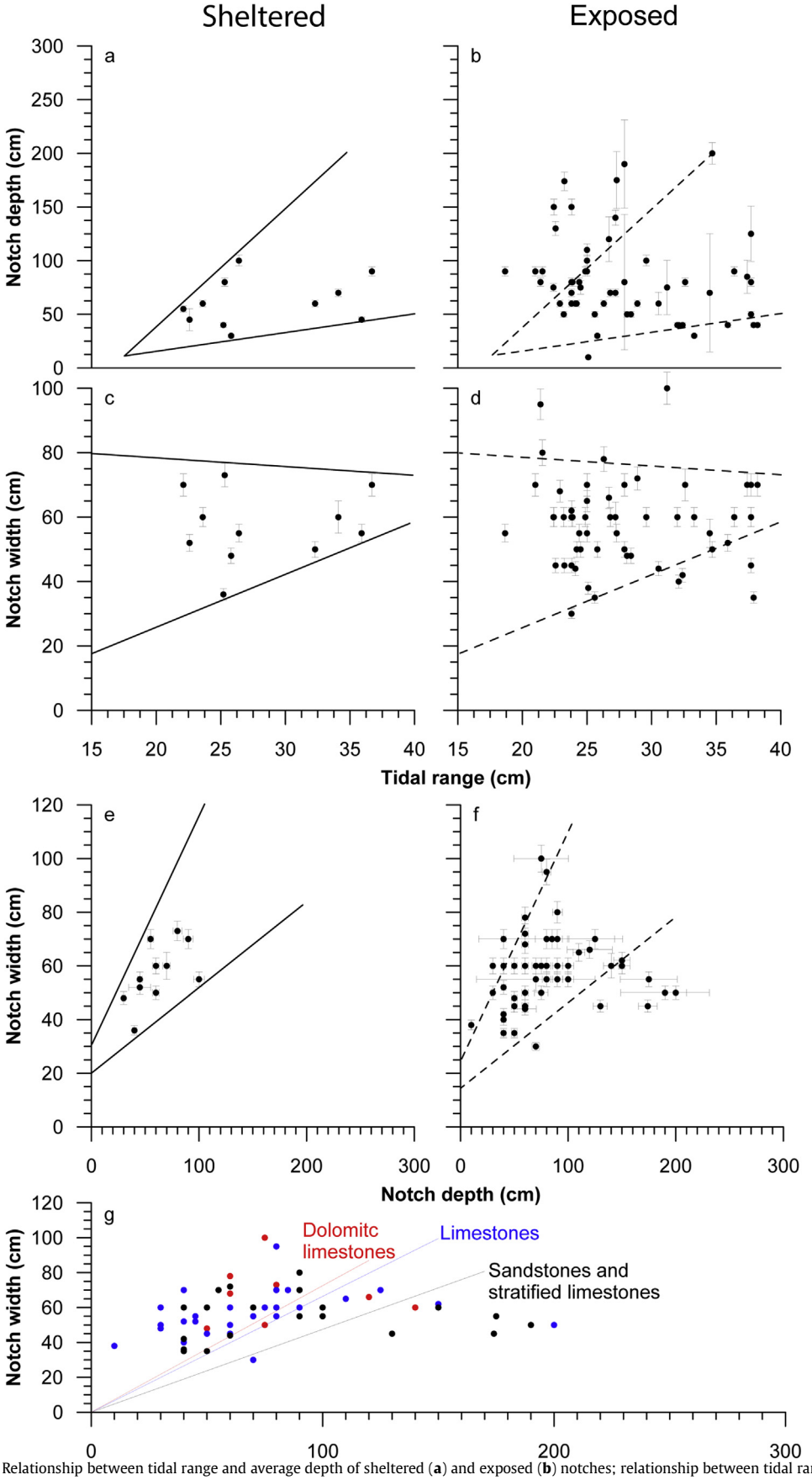

Fig. 8. Statistical diagrams. Relationship between tidal range and average depth of sheltered (**a**) and exposed (**b**) notches; relationship between tidal range and width of sheltered (**c**) and exposed (**d**) notches; relationship between average width and depth of sheltered (**e**) and exposed (**f**) notches; **g)** relationship between tidal notches and the lithology of the rock where they are carved.

4.3. Thickness of the biological rim and wave energy

It is difficult to quantify the role exerted by the wave action on the genesis of MTNs because waves have both a direct (mechanical impact) and an indirect (rim growth) action on notch development. At each site, we investigated the relationship between rim thickness (measured at the notch base), and wave energy (kw/m) reaching the coast. We excluded from computation the sites located in sheltered settings.

It is evident from Fig. 5d there is a direct correlation between rim thickness and wave energy. In general, the higher the wave energy hitting the coast, the thicker is the rim. At some sites (Badisco, Biddiriscottai, Cala Fuili, Fig. 6), and also at sites from outside the Mediterranean area (Fig. 9b, Barbados) one or more

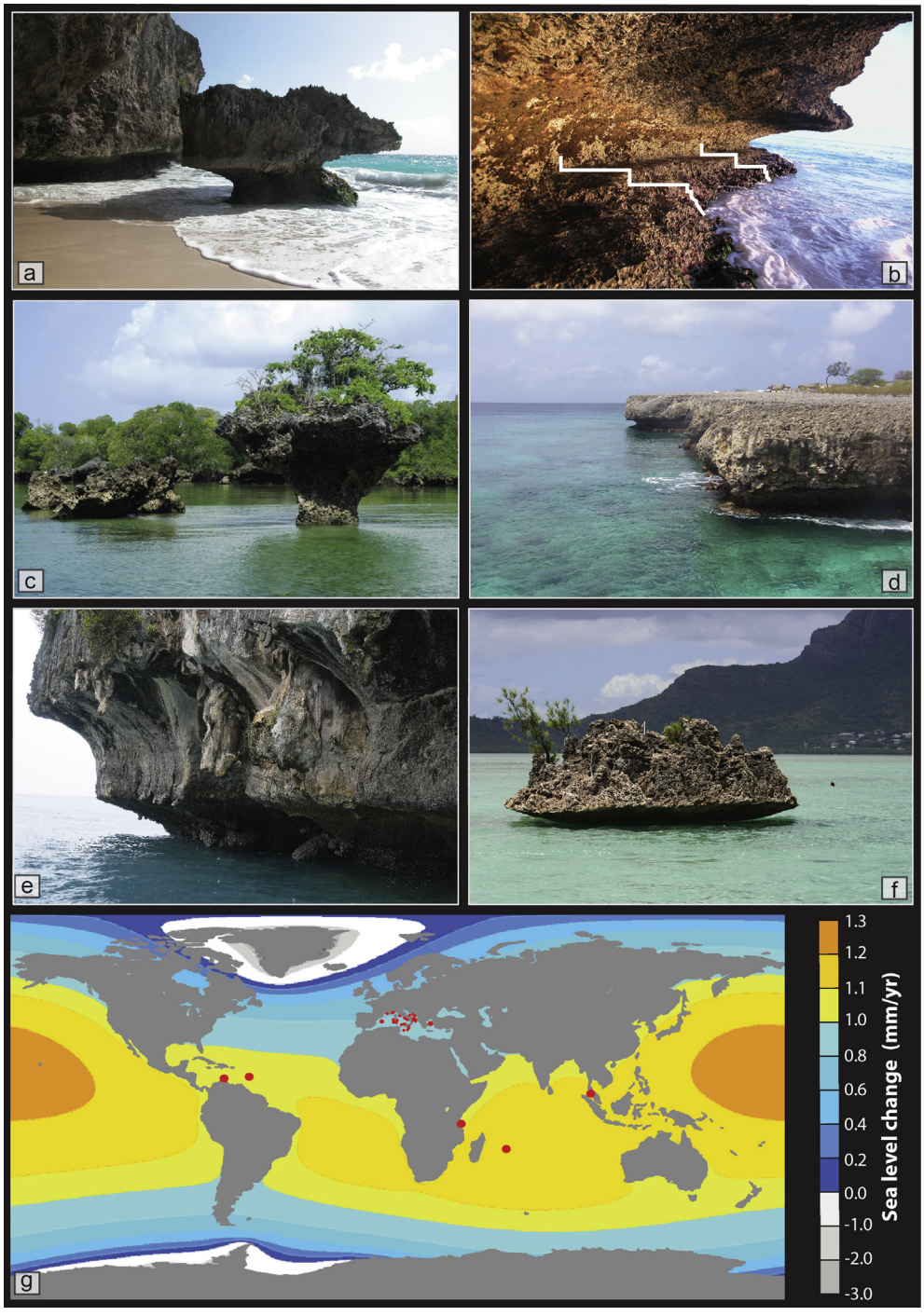

Fig. 9. Extra Mediterranean tidal notches: **a)** Barbados, notch width: 140 cm, **b)** Barbados, presence of reef steps, **c)** Zandibar, notch width: more than 400 cm, **d)** Bonaire, Netherland Antille, notch width: 100 cm, **e)** Thailand: a smoothed mid Holocene (Sheffer et al., 2012, +2.6 m 5.5 ka cal BP) notch 310 cm width and the Present day MTN, 210 cm width, **f)** Mauritius; notch width 150 cm, **g)** world wide distribution of our observations, redrawn from: Church et al., 2013 (IPCC report).

Table 4
Extra Mediterranenan Present day notches width, depth and tide prediction. For the tide prediction on the sites 1, 2, 3, 4, 5 we used: http://www.tide-forecast.com/, for sites 6 and 7 we used the original local tide gauge data.

N.	Site	Coordinates	Notch width (cm)	Notch depth (cm)	Predicted tide (cm)
1	Barbados	13° 20′ 03″ N 59° 36′ 47″W	140	210	115
2	Zanzibar Tanzania	06° 22′ 38″ S 39° 17′ 03″ E	400	200	410
3	Zanzibar Tanzania	06° 21′ 14″ S 39° 18′ 16″ E	400	400	410
4	Bonaire, Netherland Antille	12° 13′ 01″ N 68 20′ 48″ N	100	120	55
5	Phi Phi Island Thailand	07° 41′ 07″N 98° 46′ 14″E	210	120	205
6	Port Louis (Mauritius)	20° 23′ 43″S 57° 46′ 36″E	110	210	45
7	Blue Bay (Mauritius)	20° 24′ 51″S 57° 20′ 14″E	150	320	33

steps (10–12 cm in size) in the *Lithophyllum* rim has been observed, whose origin is still to be understood.

5. Discussion

5.1. Model of notch evolution

In order to explore the relations between the shape of the notch and the Holocene sea-level rise, we developed a conceptual model of notch evolution through time. This model takes into account the variability in the rate of Holocene sea-level rise (including isostatic adjustment effects, Fig. 10a). According to this model, we suggest that the shaping of the MTN started when sea level rise rate sharply decreased, 6.8 ka. Cal. BP (Lambeck et al., 2011). This flex in the relative sea-level (RSL) curve has been widely recognized in the Mediterranean Sea, and is independent of the location (and thus from the glacio-isostatic component). As an example, we show in Fig. 10a the RSL curve for Trieste, which has a minor glacio-isostatic contribution when compared to other coastal sites from the Mediterranean Sea (blue line in Fig. 10a), and the RSL curve for Cagliari (SE Sardinia, purple line in Fig. 10a), which, conversely, has a larger glacio-isostatic contribution. A sharp decrease in RSL rise is evident in both curves (5.6 and 7.36 mm/yr, respectively, between 8.0 and 6.8 ka cal BP; 0.6 and 1.42 mm/yr between 6 and 2 ka cal BP, 0.27 and 0.78 mm/yr cal BP between 2 ka and the past century, when the RSL rise increases to 1.25 mm/yr).

Therefore, the tidal notch was firstly shaped 6.8 ka. ago. This is in agreement with the database published by Boulton and Stewart (2015) (Fig. 10b), where the oldest uplifted notches are always younger than 6.5 ka. Fig. 10a shows that at coastal sites with relatively uneven glacio-isostatic contribution, the oldest MTN is predicted to be located at different depths (−4 m b.s.l. at Trieste compared to −10 m at Cagliari). Isostatic processes therefore play an important role on conditions leading to notch formation: tide gauges at Cagliari, Trieste and Genova record slightly different ranges. The rate increase observed during the last century in the RSL rise, and the past and present notch evolution, suggest that MTNs will continue to form when the RSL rise will be >1.42 mm/yr and until it will not exceed 5.6 mm/yr, the rate existing before 6.8 ka (Fig. 10a).

As sea level rose from its position 6.8 ka ago to the present level, cliffs slowly retreated and tidal notches tracked the sea level rise (Fig. 10c). In geologically stable areas, older notches are not preserved above −10 m b.s.l. because the continued sea-level rise and the accompanying abrasion led to destructive retreat of the sea-cliff. This may be the reason why submerged tidal notches are not detected in stable sites, and, conversely, they are found in uplifting (Fig. 2h) or subsiding (Fig. 2d) coasts.

The rapid dissolution and destruction of the rocky coast is testified by the characteristic “nose” (Figs. 10c and 6). Where the organic rim (mainly coralline algae and Vermetid reefs) covers the bedrock and shelters it from dissolution and abrasion, the cliff retreat is halted, as documented by the morphology of fossil notches dating more than 6 ka The Last Interglacial notch, well preserved only when sheltered by younger deposits, observed today at 4–7 m a.s.l., shows on average a larger width (10–15 cm) than the modern notch. This difference is attributed to the existence of a rim which conceals the floor of present notches and partly alter its size (Fig. 2g, f).

As shown in Fig 10c, the notch evolution allows a retreat of the cliff of at least 3 m or more for the last 6.8 ka.

5.2. Sites where the notch is missing

In rare occasions the MTN does not form (e. g. where beds have vertical dips, Fig. 11a), or it is not preserved (it is discontinuous when carved in bioclastic calcarenites, Fig. 11c,d, where it attains a 4–5 m depth and then collapses) in carbonate rocks. Besides, we did not observe the notch at the Circeo promontory (Fig. 11b) and at Capri island (Table 2).

At Circeo, where the Last Interglacial notch is also absent, the coast is crowded of colonies of Mytilus and large Balanids. We make the hypothesis that the local biocoenosis acts against notch development. In addition, large fresh-water springs do not exist at this coast (Civita, 2008). At Capri, instead, the Last Interglacial notch is well and continuously developed (Ferranti and Antonioli, 2007), but the present notch does not exist (only a wide *Lithophyllum* rim is observed at few sites), because fresh water spring with a $\geq$1000 m^3/sec flow are absent. Of course, the remarkable development of the Last Interglacial notch suggests that important springs or fresh water flows existed during the MIS 5, although this hypothesis is contrasted by the observation that the island perimeter was similar to the present one based on the development of the Last Interglacial notch. This conundrum needs still to be resolved.

5.3. Present-day formation of the notch

Based on work carried out along Greek coastlines (Euboea gulf, Corinth gulf, Cycladic islands), Evelpidiou et al. (2012) have argued that the tidal notch has been ‘drowned’ because of bioerosion (at rates between 0.3 and 1.28 mm/yr) cannot cope with the rate of sea-level rise during the last century (~1.4 mm/yr). Conversely, we have shown that the current notch is present in the vast majority of stable carbonate coasts in the central Mediterranean. We believe that the different results and interpretation between Evelpidou et al. (2012) and this paper arise from methodological aspects,

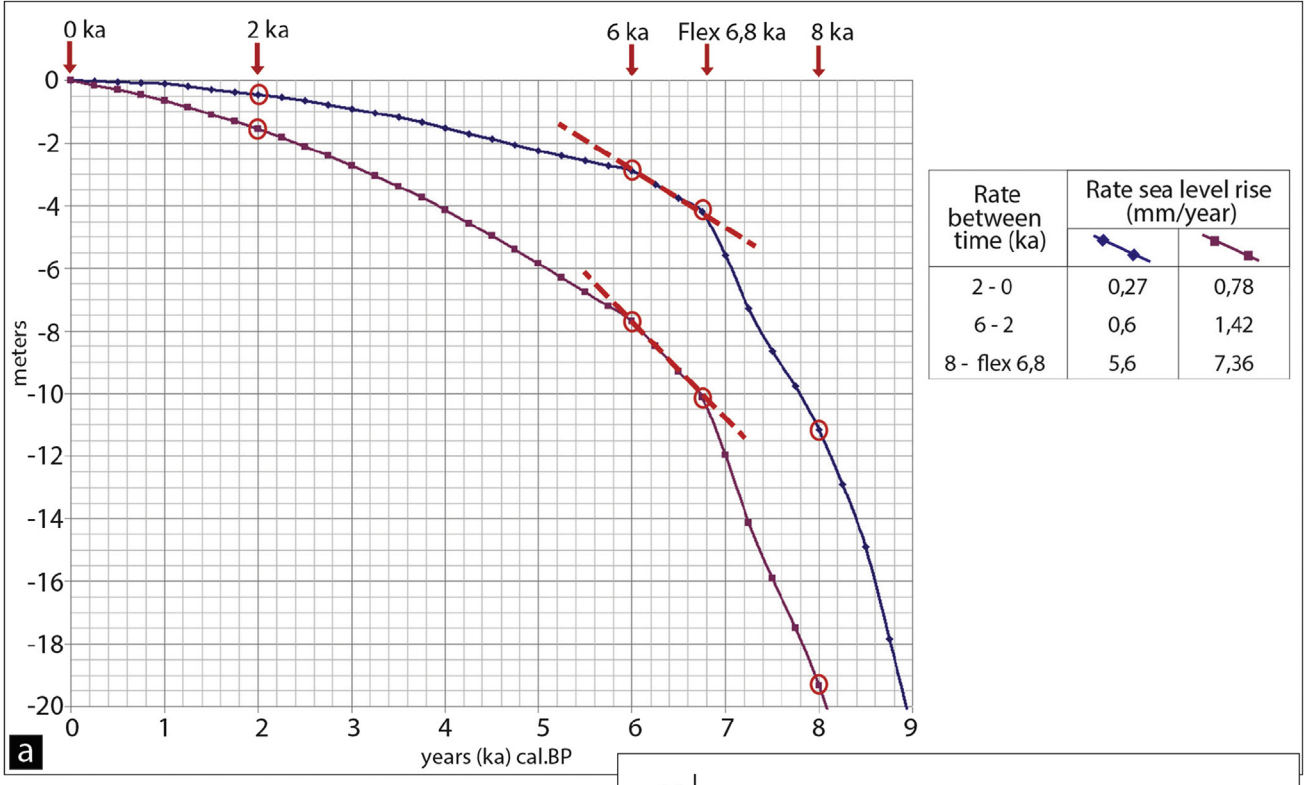

Rate between time (ka)	Rate sea level rise (mm/year)	
2 - 0	0,27	0,78
6 - 2	0,6	1,42
8 - flex 6,8	5,6	7,36

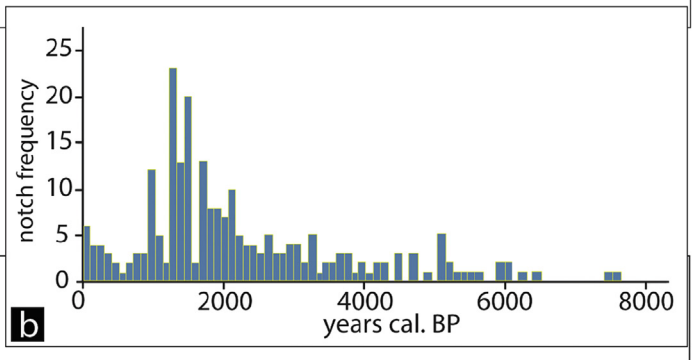

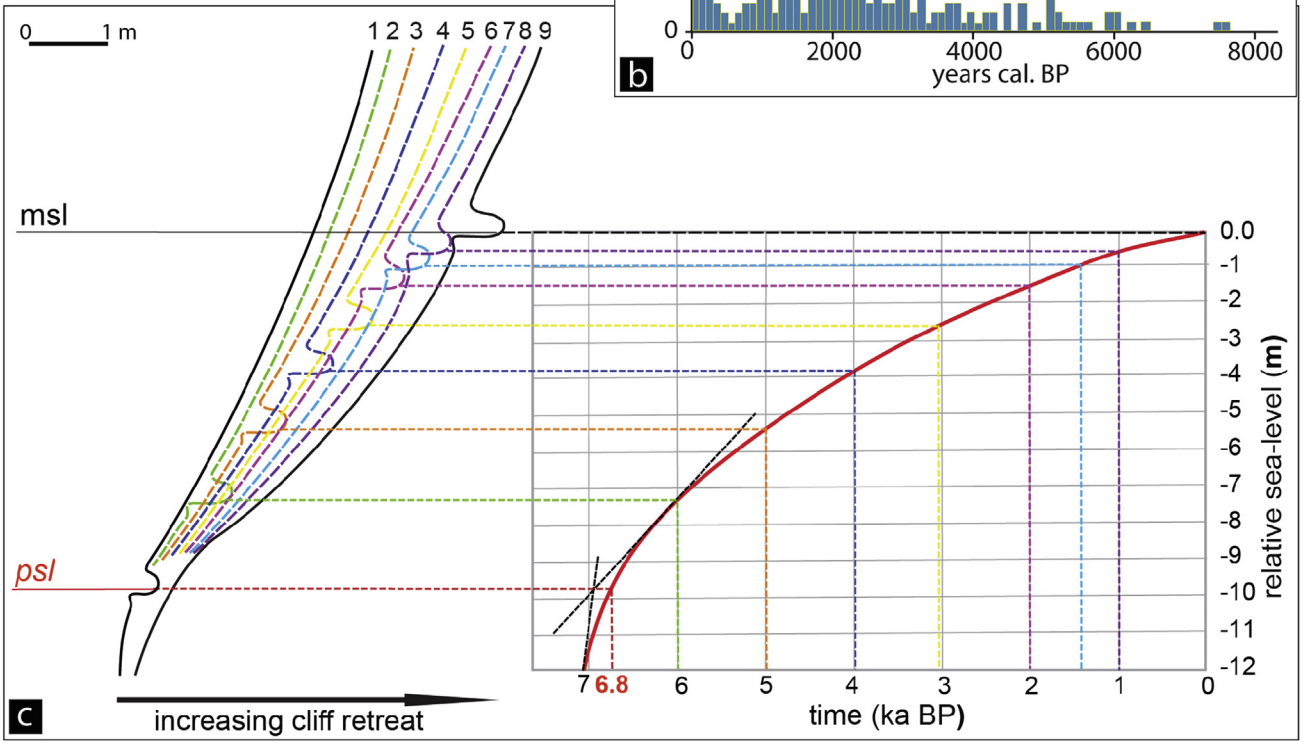

Fig. 10. **a)** Sea level rise rates from 8 ka cal BP to the Present using the predicted sea level rise curves (Lambeck model, 2011) with maximum (Cagliari, purple line) and minimum (Trieste, blue line) isostatic subsidence values. The inflection at 6.8 ka marks the change of rise. **b)** Frequency of notches formation from 8 ka to 0 ka (modified from Boulton and Stewart, 2015). **c)** Model of tidal notches formation from 6.8 ka to the present. (For interpretation of the references to colour in this figure legend, the reader is referred to the web version of this article.)

Fig. 11. Absence of tidal notches: **a)** Sardegna: the nearly vertical strata slope does not allow the formation of the notch; **b)** Circeo, Italy, molluscs (*mytilus*) create a very dense concretion. Evolution of tidal notches: **c)** Barbados, exceptionally developed tidal notches, **d)** collapse of the upper part of tidal notches.

from the uneven role attributed to specific processes concurring in notch formation, and from the proper choice of the investigated area.

Firstly, the bioerosion rate estimates are very few and scattered, when compared to the capillary distribution of available tide-gauge data worldwide, and thus generalizing erosion rates obtained in different areas for a specific area may be biased. In addition, the Authors neglect any possible contribution from different processes at local and regional scale, and namely tectonics and isostatic movements. However, the Greenland Ice Sheet contribution to the relative sea-level rise is significant and produces different responses at distant coasts with respect to the rising eustatic sea (e.g. Fig. 10a). In turn, this may have varied feedbacks on the rate of local processes, such as mechanical erosion and bioerosion.

Probably, the most important aspect creating different observations and interpretations relates to the tectonic setting of investigated sites. Greece is located on an active subduction zone and back-arc basin, where tectonic processes are very rapid and widespread. Coastal studies have shown that the Greece coastlines exhibit significant vertical tectonic movements, with abrupt transitions between subsiding, uplifting and stable sectors (Vacchi et al., 2012; Anzidei et al., 2014; with references). In contrast, Italy, apart from Calabria and the northern Adriatic sea can be considered stable or affected by very low tectonic motions at least since the MIS 5.5 (Ferranti et al., 2006, 2010; Antonioli et al., 2009). We believe that tectonic stability is a mandatory condition for a correct investigation of the origin of notches.

6. Conclusions

Careful measurement of the tidal notch geometry coupled to quantitative and qualitative investigation of processes occurring at the intertidal zone in the central Mediterranean Sea has revealed that the genesis of the notch is, rather than the effect of a single mechanism, the result of several processes that concur with different rates to the lowering of the cliff. As an example, we showed that the depth of the notch increases in exposed with respect to sheltered coastal sites. In addition, notches have slightly larger average concavity on rocky headlands and pillars, than on extended cliffs, because on the former, exposed settings, dissolution and abrasion occur with enhanced energy. On the other hand, the width of the notch seems correlated to the tidal range, and not to exposure to incoming waves. These observations suggest that exposure to wave action and tidal range are intimately intertwined in notch genesis and evolution, but act in different modes.

Another example regards the role played by encrusting organisms. While bioerosion is surely an important factor in notch development, we also show that bioprotection by the encrusting cap seems to work more effectively in areas where the wave energy is higher, and therefore constitutes a negative feedback on notch formation. In some cases, these competing processes are not enough to initiate notch formation.

However, one of the main factors leading to notch development is the existence of submarine fresh-water springs which enhance rock dissolution. Although the quantitative contribution of each single process cannot be disentangled because of the existence of mutual feedbacks between them, we stress that only an integrated appraisal of all these processes can explain the appearance and size of tidal notches at different sites. Considering only one process (Evelpidou et al., 2012) may lead to wrong conclusions.

Notwithstanding the current sea-level rise at 1.24 mm/yr in the Mediterranean Sea, the presence of the modern notch is confirmed by our observations. We explained the genesis of the modern notch with a process involving continuous carving of the notch during cliff retreat (Fig. 10c). During its evolution over the last 6.8 ka, tidal notches have undergone a continuous change in shape tracking the sea level rise and isostatic (negative) movements causing the cliff

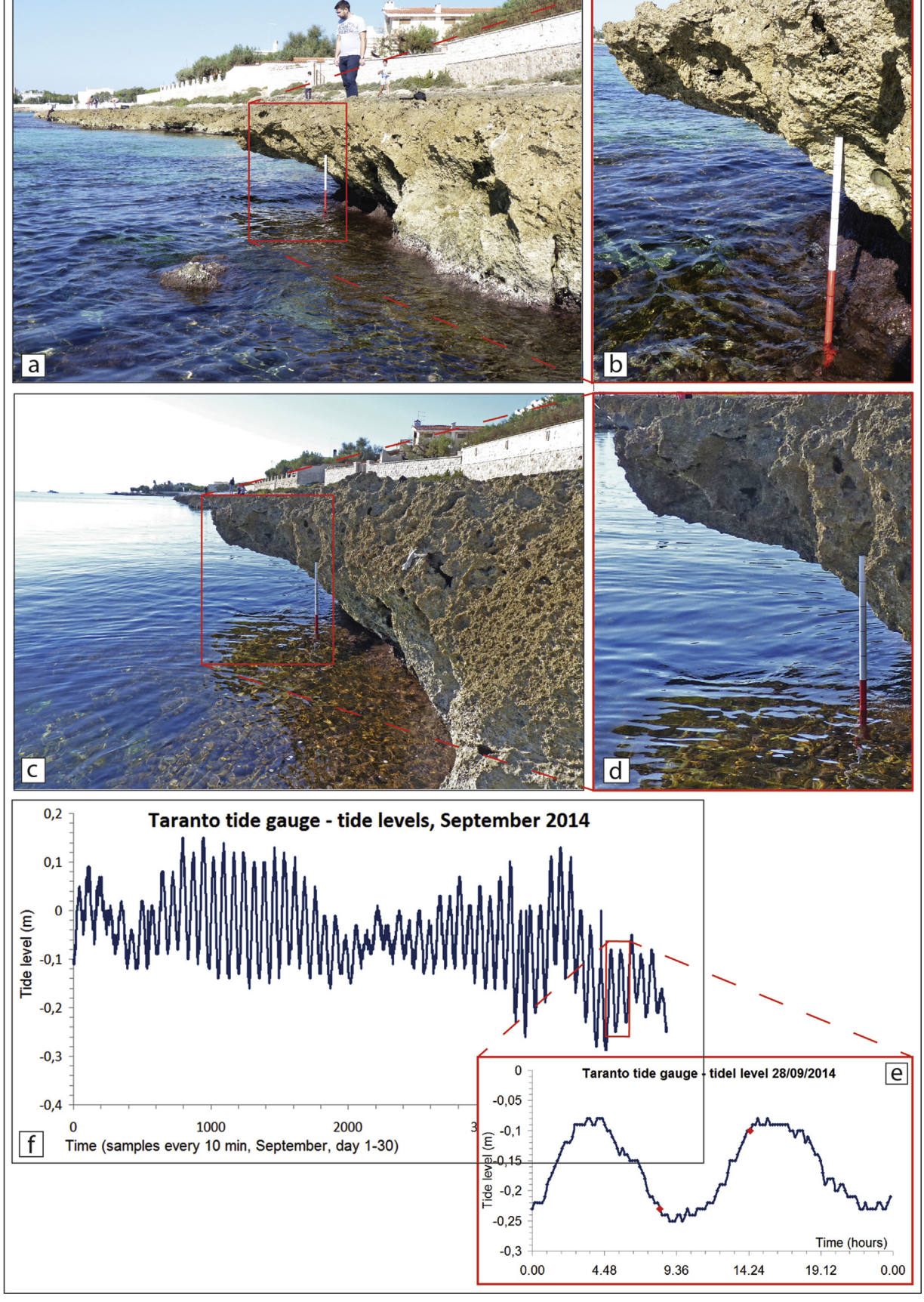

Fig. 12. Tidal range measured on the Taranto – San Vito notch (site 68 Table 1 and S1. Measured on 09/28/2014 at 10.00 am (a,b), and 16.30 pm (c,d). Observations are in agreement with the instrumental data collected at the nearest tide gauge located at Taranto. Plots show the daily tide during the observations (e) while in f) are the tides for one month cycle of September. The red arrow indicate the time of the notch measures (a,b,c,d). (For interpretation of the references to colour in this figure legend, the reader is referred to the web version of this article.)

retreat. This is the reason why submerged tidal notches are not detected in stable sites, and, conversely, tidal notches are found in uplifting (Fig. 2h) or subsiding (Fig. 2d) coasts.

The width of the Last Interglacial and the modern notches is similar, suggesting that at the vast majority of investigated sites, where both notches are present, processes have not changed during the last 125 ka. This observation indicates that long-term and large-scale oceanographic and geological processes rather than short-term processes are effective in the genesis of the notch. Finally, the local tide amplitude is always less than the tidal notch width, and the maximum notch concavity does not correspond to the maximum tidal ranges (Fig. 12).

Acknowledgements

This work has been partially funded by the Flagship Project RITMARE, by the COFIN MIUR 2010–2011 "*Response of morphoclimatic system dynamics to global changes and related geomorphological hazard*", and carried out under the umbrella of the Medflood project (INQUA project 1203P) and of the IGCP Project n. 588 from UNESCO – IUGS. AR wants to thank the Institutional Strategy of the University of Bremen, funded by the German Excellence Initiative, and ZMT the Leibniz Center for Tropical Marine Ecology.

Appendix A. Supplementary data

Supplementary data related to this article can be found at http://dx.doi.org/10.1016/j.quascirev.2015.03.016.

References

Alpert, P., Baldi, M., Ilani, R., Krichak, S., Price, C., Rodò, X., Saaroni, H., Ziv, B., Kishcha, P., Barkan, J., Mariotti, A., Xoplaki, E., 2006. Relations between climate variability in the Mediterranean region and the Tropics: ENSO, South Asian and African monsoons, hurricanes and Saharan dust. In: Lionello, P., Malanotte-Rizzoli, P., Boscolo, R. (Eds.), Mediterranean Climate Variability. Amsterdam, pp. 145–172.

Anzidei, M., Lambeck, K., Antonioli, F., Furlani, S., Mastronuzzi, G., Serpelloni, E., Vannucci, G., 2014. Coastal Structure, Sea-level Changes and Vertical Motion of the Land in the Mediterranean. In: Geological Society, London, Special Publications, vol. 388. http://dx.doi.org/10.1144/SP388.20.

Anzidei, M., Antonioli, F., Lambeck, K., Benini, A., Soussi, M., Lakhdar, R., 2011. New insights on the relative sea level change during Holocene along the coasts of Tunisia and western Libya from archaeological and geomorphological markers. Quat. Int. 232, 5–12.

Antonioli, F., Carulli, G.B., Furlani, S., Auriemma, R., Marocco, R., 2004. The enigma of submerged marine notches in northern Adriatic Sea. Quaternaria VIII, 27–36.

Antonioli, F., Anzidei, M., Lambeck, K., Auriemma, R., Gaddi, D., Furlani, S., Orrù, P., Solinas, E., Gaspari, A., Karinja, S., Kovačić, V., Surace, L., 2007. Sea level change during Holocene from Sardinia and northeastern Adriatic (Central Mediterranean sea) from archaeological and geomorphological data. Quat. Sci. Rev. 26, 2463–2524.

Antonioli, F., Ferranti, L., Fontana, A., Amorosi, A.M., Bondesan, A., Braitenberg, C., Dutton, A., Fontolan, G., Furlani, S., Lambeck, K., Mastronuzzi, G., Monaco, C., Spada, G., Stocchi, P., 2009. Holocene relative sea-level changes and vertical movements along the Italian coastline. Quat. Int. 221, 37–51.

Bonacci, O., Ljubenkov, I., Roje-Bonacci, T., 2006. Karst flash floods: an example from the Dinaric karst (Croatia). Nat. Hazards Earth Syst. Sci. 6, 195–203.

Boulton, S.J., Stewart, I.S., 2015. Holocene Coastal Notches in the Mediterranean Region: indicators of Palaeoseismic clustering? Geomorphology 237, 29–37. http://dx.doi.org/10.1016/j.geomorph.2013.11.012.

Carobene, L., 1972. Osservazioni sui solchi di battente attuali ed antichi nel Golfo di Orosei in Sardegna. Mem. della Soc. Geol. Ital. 19, 641–649.

Cavaleri, L., Bertotti, L., Lionello, P., 1991. Wind wave cast in the Mediterranean Sea. J. Geoph. Res. 98 (C8), 10739–10764.

Cavaleri, L., 2000. The oceanographic tower Acqua Alta – activity and prediction of sea states at Venice. Coast. Eng. 39, 29–70.

Channell, J.E.T., Horvath, F., 1976. The African-Adriatic promontory as a paleogeographical premise for Alpine orogeny and plate movements in the Carpatho-Balkan regional. Tectonophysics 35, 71–110.

Civita, M.V., 2008. L'assetto idrogeologico del territorio italiano: risorse e problematiche. Quad. SGI 3, 4–32.

Cooper, F.J., Roberts, G.P., Underwood, C.J., 2007. A comparison of 103-105 climate stability and the formation of coastal notches. Geophys. Res. Lett. 34, L14310. http://dx.doi.org/10.1029/2007GL030673.

Church, J.A., Clark, P.U., Cazenave, A., Gregory, J.M., Jevrejeva, S., Levermann, A., Merrifield, M.A., Milne, G.A., Nerem, R.S., Nunn, P.D., Payne, A.J., Pfeffer, W.T., Stammer, D., Unnikrishnan, A.S., 2013. Sea level change. In: Stocker, T.F., Qin, D., Plattner, G.-K., Tignor, M., Allen, S.K., Boschung, J., Nauels, A., Xia, Y., Bex, V., Midgley, P.M. (Eds.), Climate Change 2013: the Physical Science Basis. Contribution of Working Group I to the Fifth Assessment Report of the Intergovernmental Panel on Climate Change. Cambridge University Press, Cambridge, United Kingdom and New York, NY, USA.

De Waele, J., Furlani, S., 2013. Seawater and biokarst effects on coastal limestones. In: Shroder, J., Frumkin, A. (Eds.), Treatise on Geomorphology, Karst Geomorphology, vol. 6. Academic Press, San Diego, CA, pp. 341–350.

Emery, K.O., 1962. Marine Geology of Guam. In: U.S. Geological Survey, Professional Paper, 403B, p. 76.

Evelpidou, N., Kampolis, I., Pirazzoli, P.A., Vassilopoulos, A., 2012. Global sea-level rise and disappearence of tidal notches. Glob. Planet. Changes 92–93, 248–256.

Faivre, S., Bakran Petricioli, T., Horvatintcic, N., 2010. Relative sea level change during the late Holocene on the Island of Vis (Croatia) Issa harbor archaeological site. Geodin. Acta 23 (5–6), 209–223.

Faivre, S., Fouache, E., Ghilardi, M., Antonioli, F., Furlani, S., Kovačić, V., 2011. Relative sea level change in Istria (Croatia) during the last 5 ka. Quat. Int. 232, 132–143.

Faivre, S., Bakran-Petricioli, T., Horvatinčić, N., Sironić, A., 2013. Distinct phases of relative sea level changes in the central Adriatic during the last 1500years – influence of climatic variations? Palaeogeogr. Palaeoclimatol. Palaeoecol. 369, 163–174.

Ferranti, L., Antonioli, F., Amorosi, A., Dai Prà, G., Mastronuzzi, G., Mauz, B., Monaco, C., Orrù, P., Pappalardo, M., Radtke, U., Renda, P., Romano, P., Sansò, P., Verrubbi, V., 2006. Elevation of the last interglacial highstand in Sicily (Italy): a benchmark of coastal tectonics. Quat. Int. 145–146, 30–54.

Ferranti, L., Antonioli, F., 2007. Misure del solco Tirreniano (MIS 5.5) nell'isola di Capri valutazione di attività tettonica durante il Pleistocene Inferiore. Il Quat. 20, 125–136.

Ferranti, L., Antonioli, F., Anzidei, M., Monaco, C., Stocchi, P., 2010. The timescale and spatial extent of vertical tectonic motions in Italy: insights from relative sea-level changes studies. J. Virtual Expl. Electron. Ed 36. Paper 30.

Flemming, N., Webb, C.O., 1986. Tectonic and eustatic coastal changes during the last 10,000 years derived from archaeological data. Z. Geomorphol. 62, 1–29.

Fleury, P., Bakalowicz, M., de Marsily, G., 2007. Submarine springs and coastal karst aquifers: a review. J. Hydrol. 339 (1), 79–92.

Furlani, S., Cucchi, F., Forti, F., Rossi, A., 2009. Comparison between coastal and inland Karst limestone lowering rates in the northeastern Adriatic Region (Italy and Croatia). Geomorphology 104, 73–81.

Furlani, S., Cucchi, F., Odorico, R., 2010. A new method to study microtopographical changes in the intertidal zone: one year of TMEM measurements on a limestone removable rock slab (RRS). Z. Geolorphol. 54 (Suppl. 2), 137–151.

Furlani, S., Cucchi, F., 2013. Downwearing rates of vertical limestone surfaces in the intertidal zone (Gulf of Trieste, Italy). Mar. Geol. 343, 92–98.

Furlani, S., Ninfo, A., Zavagno, E., Paganini, P., Zini, L., Biolchi, S., Antonioli, F., Coren, F., Cucchi, F., 2014a. Submerged notches in Istria and the Gulf of Trieste: results from the Geoswim Project. Quat. Int. 332, 37–47.

Furlani, S., Pappalardo, M., Gomez-Pujol, L., Chelli, A., 2014b. Mediterranean and Black Sea. In: Kennedy, D.M., Stephenson, W.J., Naylor, L. (Eds.), Rock Coast Geomorphology. A Global Synthesis, Geological Society, London, Memoirs, 40, pp. 89–123.

Galili, E., Sevketoglu, M., Salamon, A., Zviely, D., Mienis, H., Rosen, B., Moshkovitz, S., 2011. Late Pleistocene beach deposits, tectonics and sea-level changes on Cyprus, and their possible association with Neolithic colonization and settlements, 2001. In: INQUA Seventh Plenary Meeting. Abstract volume, 84–85.

Gary, D., Egbert, Svetlana, Y., Erofeeva, 2002. Efficient Inverse modeling of Barotropic Ocean Tides. J. Atmos. Ocean. Technol. 19, 183–204.

Giorgi, F., Lionello, P., 2008. Climate change projections for the Mediterranean region. Glob. Planet. Change 63, 90–104.

Higgins, C.G., 1980. Nips, Notches, and the Solution of Coastal Limestone: an overview of the problem with examples from Greece. Estuar. Coast. Sci. 10, 15–30.

Jolivet, L., Faccenna, C., 2000. Mediterranean extension and the Africa-Eurasia collision. Tectonics 19 (6), 1095–1106.

Kanyaya, J.I., Trenhaile, A.S., 2005. Tidal wetting and drying on shore platforms: an experimental assessment. Geomorphology 70, 129–146.

Kaye, C.A., 1957. The effect of solvent motion on limestone solution. J. Geol. 65, 35–46.

Kelletat, D.H., 2005. Notches. In: Schwartz, M.L. (Ed.), Encyclopedia of Coastal Science. Springer, Dordrecht, pp. 728–729.

Kleypas, J.A., Buddemeier, R.W., Archer, D., Gattuso, J.P., Langdon, C., Opdyke, B.N., 1999. Geochemical consequences of increased atmospheric carbon dioxide on coral reefs. Science 284, 118.

Laborel, J., Peres, J.M., Picard, J., Vacelet, J., 1961. Etude directe des fonds des parages de Marseille de 30 a 300m avec la soucoupe plongeante Cousteau. Bull. Inst. Oceanogr. Monaco 1206, 1–16.

Laborel, J., Laborel-Deguen, F., 1996. Biological indicators of Holocene sea-level and climatic variations on rocky coasts of tropical and subtropical regions. Quat. Int. 31, 53–60.

Lambeck, K., Antonioli, F., Anzidei, M., Ferranti, L., Leoni, G., Scicchitano, G., Silenzi, S., 2011. Sea level change along the Italian coast during the Holocene and projections for the future. Quat. Int. 232 (1–2), 250–257.

Le Campion-Alsumard, T., 1979. Les cyanophycées endolithes marines. Systématique, ultrastructure, écologie et biodestruction. Oceanol. Acta 2, 143–156.
Liberti, L., Carillo, A., Sannino, G., 2013. Wave energy resource assessment in the Mediterranean, the Italian perspective. Renew. Energy 50, 938–949. http://utmea.enea.it/projects/energiadalmare/.
Lionello, P., Bhend, J., Buzzi, A., Della-Marta, P.M., Krichak, S., Jansà, A., Maheras, P., Sanna, A., Trigo, I.F., Trigo, R., 2006. Cyclones in the Mediterranean region: climatology and effects on the environment. In: Lionello, P., Malanotte-Rizzoli, P., Boscolo, R. (Eds.), Mediterranean Climate Variability. Elsevier, Amsterdam, pp. 324–372.
MacFadyen, W.A., 1930. The undercutting of coral reef limestone on the coasts of some islands in the Red Sea. Geogr. J. 75, 27–34.
Morton, B., Scott, P.J.B., 1980. Morphological and functional specializations of the shell, musculature and pallial glands in the Lithophaginae (Mollusca: Bivalvia). J. Zool. 192, 179–203.
Naylor, L.A., Viles, H.A., 2002. A new technique for evaluating short-term rates of coastal bioerosion and bioprotection. Geomorphology 47, 31–44.
Naylor, L.A., Coombes, M.A., Viles, H.A., 2012. Reconceptualising the role of organisms in the erosion of rock coasts: a new model. Geomorphology 157–158, 17–30.
Oldow, J.S., Ferranti, L., Lewis, D.S., Campbell, J.K., D'Argenio, B., Catalano, R., Pappone, G., Carmignani, L., Conti, P., Aiken, C.L.V., 2002. Active fragmentation of Adria based on Global Positioning System velocities and regional seismicity. Geology 30, 779–782.
Pavlopoulos, K., Kapsimalis, V., Theodorakopoulou, K., Panagiotopoulos, I.P., 2012. Vertical displacement trends in the Aegean coastal zone (NE Mediterranean) during the Holocene assessed by geo-archaeological data. Holocene 22, 717–728.
Peyrot-Clausade, M., Chabanet, P., Conand, C., Fontaine, M.F., Letourneur, Y., Harmelin-Vivien, M., 2000. Sea urchin and fish bioerosion on La Reunion and Moorea reefs. Bull. Mar. Sci. 66, 477–485.
Pirazzoli, P.A., 1986. Marine notches. In: van de Plassche, O. (Ed.), Sea-level Research: a Manual for the Collection and Evaluation of Data. Geo Books, Norwich, pp. 361–400.
Pirazzoli, P.A., 1991. World Atlas of Holocene Sea-level Changes. Elsevier, Amsterdam, p. 300.
Pirazzoli, P.A., Stiros, S.C., Laborel, J., Arnold, M., Papageorgiou, S., Morhange, C., 1994. Late-Holocene shoreline changes related to palaeoseismic events in the Ionian Islands, Greece. Holocene 4, 397.
Pirazzoli, P.A., Evelpidou, N., 2013. Tidal notches: a sea-level indicator of uncertain archival trustwothiness. Palaeogeogr. Palaeoclimatol. Palaeoecol. 369, 377–384.
Poulos, S.E., Ghionis, G., Maroukian, H., 2009. Sea-level rise trends in the Attico Cycladic region (Aegean Sea) during the last 5000 years. Geomorphology 107, 10–17.
Radic Rossi, I., Antonioli, F., 2008. Preliminary Considerations on the ancient Port of Pakostane (Croatia) based on archaeological and Geomorphologic Research. In: European Association of Archaeologists, Malta 14th Annual Meeting. Abstract volume 43–44.
Rebora, N., Molini, L., Casella, E., Comellas, A., Fiori, E., Pignone, F., Siccardi, F., Silvestro, F., Tanelli, S., Parodi, A., 2013. Extreme rainfall in the mediterranean: what can we learn from observations? J. Hydrometeorol. 14 (3), 906–922.
Rodríguez-Vidal, J., Abad, M., Cáceres, L.M., Ruiz, F., Fa, D.A., Finlayson, C., Finlayson, G., Martínez Aguirre, A., 2007. Evidencias erosivos y bioerosivas en la costa rocosa de Gibraltar al inicio del último interglacial. In: Gómez-Pujol, L., Fornós, J.J. (Eds.), Investigaciones Recientes (2005–2007) en Geomorfología Litoral. UIB, IMEDEA, SHNB, SEG, ISBN 978-84-611-5926-0, pp. 197–201.
Royden, L.H., Papanikolaou, D.J., 2011. Slab segmentation and late Cenozoic disruption of the Hellenic arc. Geochem. Geophys. Geosyst. 12, Q03010. http://dx.doi.org/10.1029/2010GC003280.
Sartoretto, S., Francour, P., 1997. Quantification of bioerosion by Sphaerechinus Granularis on 'corraligene' concretions of the western Mediterranean. J. Mar. Biol. Ass. U. K. 77, 565–568.
Serpelloni, E., Vannucci, G., et al., 2007. Kinematics of the Western Africa–Eurasia plate boundary from focal mechanisms and GPS data. Geophys. J. Int. 169, 1180–1200.
Spencer, T., Viles, H.A., 2002. Bioconstruction, bioerosion and disturbance on coral reefs and rocky carbonate coasts. Geomorphology 48, 23–50.
Stanley, J.D., Toscano, M.A., 2009. Ancient archaeological sites Buried and submerged along Egypt's Nile Delta Coast: gauges of Holocene Delta Margin Subsidence. J. Coast. Res. 25 (1), 158–170.
Stephenson, W.J., Kirk, R.M., 2000. Development of shore platforms on Kaikoura Peninsula, South Island, New Zealand: II: the role of subaerial weathering. Geomorphology 32 (1), 43–56.
Stewart, I.S., Morhange, C., 2009. Coastal geomorphology and sea-level change. In: Woodward, J.C. (Ed.), The Physical Geography of the Mediterranean. Oxford University Press, Oxford, pp. 385–413.
Sulli, A., Lo Presti, V., Gasparo Morticelli, M., Antonioli, F., 2013. Vertical movements in NE Sicily and its offshore: outcome of tectonic uplift during the last 125 ky. Quat. Int. 288, 168–182.
Taborosi, D., Kázmér, M., 2013. Erosional and depositional textures and structures in coastal karst landscapes. In: Lace, M.J., Mylroie, J. (Eds.), (szerk.) Coastal Karst Landforms. Springer Science+Business Media, Dordrecht, pp. 15–58.
Torunski, H., 1979. Biological erosion and its significance for the morphogenesis of limestone coasts and for nearshore sedimentation (northern Adriatic). Senckenberg. Maritima 11 3 (6), 193–265.
Trenhaile, A.S., Mercan, D.W., 1984. Frost weathering and the saturation of coastal rocks. Earth Surf. Process. Landforms 9, 321–331.
Trenhaile, A.S., 2002. Rock coasts, with particular emphasis on shore platform. Geomorphology 48, 7–22.
Trenhaile, A.S., Porter, N.J., 2007. Can shore platforms be produced solely by weathering processes? Mar. Geol. 241, 79–92.
Trenhaile, A.S., 2014. Modelling marine notch formation by wetting and drying and salt weathering. Geomorphology 224, 139–151.
Tsimplis, M., Spada, G., Marcos, M., Flemming, N., 2011. Multi-decadal sea level trends and land movements in the Mediterranean Sea with estimates of factors perturbing tide gauge data and cumulative uncertainties. Glob. Plan. Change 76, 63–76.
Vacchi, M., Rovere, A., Zouros, N., Desruelles, S., Caron, V., Firpo, M., 2012. Spatial distribution of sea-level markers on Lesvos Island (NE Aegean Sea): evidence of differential relative sea-level changes and the neotectonic implications. Geomorphology 159–160, 50–62.
Verstappen, H.Th, 1960. On the geomorphology of raised coral reefs and its tectonic significance. Z. Geomorphol. N. F. 4, 1–28.
Vött, A., 2007. Relative sea level changes and regional tectonic evolution of seven coastal areas in NW Greece since the mid-Holocene. Quat. Sci. Rev. 26, 894–919.
Yaltirak, C., Sakinc, M., Aksu, A.E., Hiscott, R.N., Galleb, B., Ulgen, U.B., 2002. Late Pleistocene uplift history along the southwestern Marmara Sea determined from raised coastal deposits and global sea-level variations. Mar. Geol. 190, 283–305.